Quaternary Science Reviews 300 (2023) 107837

Contents lists available at ScienceDirect

Quaternary Science Reviews

journal homepage: www.elsevier.com/locate/quascirev

Tropical Indian Ocean basin hydroclimate at the Mid- to Late-Holocene transition and the double drying hypothesis

Nick Scroxton [a, b, *], Stephen J. Burns [a], David McGee [b], Laurie R. Godfrey [c], Lovasoa Ranivoharimanana [d], Peterson Faina [d], Benjamin H. Tiger [b, e]

[a] Department of Geosciences, 611 North Pleasant Street, University of Massachusetts Amherst, MA 01030, USA
[b] Department of Earth, Atmospheric and Planetary Sciences, Massachusetts Institute of Technology, 77 Massachusetts Avenue, Cambridge, MA 02139, USA
[c] Department of Anthropology, 240 Hicks Way, University of Massachusetts, Amherst, MA 01003, USA
[d] Mention Bassins Sédimentaires, Evolution, Conservation (BEC) – BP 906 – Faculté des Sciences, Université D'Antananarivo – 101 Antananarivo, Madagascar
[e] Woods Hole Oceanographic Institution, 266 Woods Hole Road, Woods Hole, MA 02543, USA

ARTICLE INFO

Article history:
Received 12 July 2022
Received in revised form
16 September 2022
Accepted 19 October 2022
Available online 24 November 2022

Handling Editor: Dr Mira Matthews

Keywords:
Holocene
Paleoclimatology
Monsoon
Indian ocean
Data synthesis
Indus valley
4.2 ka event
Harappan

ABSTRACT

The spatial pattern of Holocene climate anomalies is crucial to determining the mechanisms of change, distinguishing between unforced and forced climate variability, and understanding potential impacts on past and future human societies. The 4.2 ka event is often regarded as one of the largest and best documented abrupt climate disturbances of the Holocene. Yet outside the data-rich Northern Hemisphere mid-latitudes, the global pattern of climate anomalies is uncertain. In this study we investigate the spatial and temporal variability of the tropical Indian Ocean hydroclimate at the Mid- to Late-Holocene transition. We conducted Monte-Carlo principal component analysis, considering full age uncertainty, on ten high-resolution, precisely dated paleohydroclimate records from around the tropical Indian Ocean basin, all growing continuously or almost continuously between 5 and 3 kyr BP. The results indicate the dominant mode of variability in the region was a drying between 3.97 kyr BP (±0.08 kyr standard error) and 3.76 kyr BP (±0.07 kyr standard error) with dry conditions lasting for an additional 300 years in some records, and a permanent change in others. This drying in PC1, which we interpret as a proxy of summer monsoon variability, fits with a previously recognised tropic wide change in hydroclimate around 4.0 kyr BP. An abrupt event from 4.2 to 3.9 kyr BP is seen locally in individual records but lacks regional coherence.

A lack of apparent 4.2 ka event in tropical Indian Ocean hydroclimate has ramifications for climate variability in the Indus valley, and for the Harappan civilization. Through a comparison of existing Indian subcontinent paleoclimate records, upstream climatic variability in the Indian Summer Monsoon and winter Westerly Disturbances source regions, and modern climatology, we present the "Double Drying hypothesis". A winter rainfall drying between 4.2 and 3.9 kyr BP was followed by a summer rainfall drying between 3.97 kyr BP and at least 3.4 kyr BP. The Double Drying hypothesis provides more detailed climatic context for the Harappan civilization, resolves the cropping paradox, and fits the spatial-temporal pattern of urban abandonment. The consequences for the new Mid- to Late-Holocene Global Boundary Stratotype Section and Point in a stalagmite from Meghalaya are explored.

1. Introduction

Understanding the spatial patterns and processes of Holocene climate variability is an important component in determining the climate system's response to perturbation under modern boundary conditions (Fleitmann et al., 2003; Gupta et al., 2003; Mayewski et al., 2004; Wanner et al., 2011). In particular, distinguishing extreme climate states caused by internal variability from small,

* Corresponding author. Irish Climate Analysis and Research Units, Department of Geography, Maynooth University, Maynooth, Co. Kildare, Ireland.
E-mail addresses: nick.scroxton@mu.ie (N. Scroxton), sburns@geo.umass.edu (S.J. Burns), davidmcg@mit.edu (D. McGee), lgodfrey@umass.edu (L.R. Godfrey), ranivolova@gmail.com (L. Ranivoharimanana), petersonfaina@gmail.com (P. Faina), tigerb@mit.edu (B.H. Tiger).

https://doi.org/10.1016/j.quascirev.2022.107837
0277-3791/

forced events is crucial when attributing extreme events to modern climate change.

In the Northern Hemisphere mid-latitudes, the 4.2 ka event (4.26–3.97 kyr BP (Carolin et al., 2019)) is one of the largest climate anomalies of the Holocene (Bini et al., 2019; Booth et al., 2005; Kaniewski et al., 2018), and was recently designated as the chronostratigraphic boundary between the Northgrippian and Meghalayan subdivisions of the Holocene epoch (Walker et al., 2018). The climatic impact and mechanisms of the 4.2 kyr BP event are best understood in the data-rich heartland of Mediterranean Europe (Bini et al., 2019) and Middle East (Kaniewski et al., 2018), where the event is manifested as a hydroclimate anomaly beginning abruptly at 4.2 kyr BP and extending until 3.97 kyr BP. Yet it remains unclear whether the 4.2 ka event is a relatively modest forced event (e.g., as a freshwater input to the North Atlantic; Wang et al., 2013), or a very large unforced event (Yan and Liu, 2019). A reduction in winter rainfall due to reduced western disturbances has been proposed as a mechanism for regional drying across the Mediterranean and Middle East (Cookson et al., 2019), although spatial heterogeneity limits a mechanistic understanding of the climate mechanisms involved (Bini et al., 2019). The 4.2 ka event also garners attention because of its synchronicity with major societal transformations (Höflmayer, 2017; Wang et al., 2016), providing test cases for exploring the role of climate in societal change (Butzer and Endfield, 2012; deMenocal, 2001; Weiss and Bradley, 2001).

Globally, numerous individual records report climatic anomalies at 4.2 kyr BP, yet the spatial and temporal pattern of the event remains unclear. This is due to poor spatial coverage of records, the use of low-resolution records with limited ability to reliably detect a 300-year anomaly, and chronological uncertainties inherent in paleoclimate records. Given these uncertainties it is likely that the 4.2 ka event may be 'found' in records because it is searched for. For example, in the tropics and monsoonal areas, climate anomalies with age uncertainties that overlap 4.26–3.97 kyr BP are often attributed to the 4.2 ka event (Marchant and Hooghiemstra, 2004; Staubwasser and Weiss, 2006). This includes dry conditions in tropical Africa (Marchant and Hooghiemstra, 2004), wet conditions in tropical South America (Marchant and Hooghiemstra, 2004), changes to ENSO (Toth and Aronson, 2019) and aridification in India (Dixit et al., 2014, 2018). Yet it is increasingly recognised that there was an abrupt change in ENSO behavior around 4.0 kyr BP with an increase in the frequency of El Niño events, and/or a narrowing of the tropical rainbelt (de Boer et al., 2014; Denniston et al., 2013; Gagan et al., 2004; Giosan et al., 2018; Li et al., 2018; MacDonald, 2011; Toth et al., 2012). It should be noted that the original literature is not always the source of attribution of climate variability to the 4.2 ka event. For example, Marchant and Hooghiemstra (2004) attributed multi-site changes to a circa 4 kyr BP change in tropical sea surface temperatures. An association with the 4.2 ka event was added later by others (e.g. Staubwasser and Weiss, 2006). Regardless, distinguishing or reconciling concurrent climate events is crucial in understanding the spatial extent of these events, and therefore their underlying mechanistic processes.

To understand the spatial extent, pattern and impact of the 4.2 ka event outside of the Mediterranean and Middle East data-rich heartland, there is a need to synthesise high quality, high resolution, precisely dated paleoclimate records using quantitative statistical techniques. In this study we focus on paleohydroclimate records from the tropical Indian Ocean basin (Fig. 1). We choose this region because: 1) there has been a recent spate of publications of high resolution paleoclimate records in the region, including new speleothem records from western India (Kathayat et al., 2017), Sumatra (Wurtzel et al., 2018), Rodrigues Island (Li et al., 2018), and Madagascar (Wang et al., 2019; Scroxton et al., 2023), and a high resolution planktonic foraminifera record from a sediment core from the Arabian Sea (Giesche et al., 2019). 2) The tropical Indian Ocean basin contains a recognised, temporally proximal, climate anomaly at 4.0 kyr BP that should be distinguishable to the 4.2 ka event in high-resolution, precisely dated records (Denniston et al., 2013). 3) Societal changes and deurbanization at the end of the Mature Harappan period occurred in and around the Indus valley between 4.2 and 3.9 kyr BP (Dixit et al., 2014; Petrie et al., 2017), and these changes are frequently attributed to a decline in summer monsoonal rainfall.

2. Methods

To investigate tropical Indian Ocean hydroclimate variability at the Mid- to Late-Holocene transition we focused on speleothem $\delta^{18}O$ records. Radiometric U–Th dating of stalagmites provides highly precise age models and high-resolution sampling is frequently at the decadal scale or better. Specifically, speleothem records had to have near-continual coverage and two U–Th ages between 5.0 and 3.0 kyr BP, and have better than 15-year sample resolution. The chosen records were from northern Australia, Oman, northwest India, Rodrigues, Sumatra and Madagascar (Denniston et al., 2013; Fleitmann et al., 2007; Kathayat et al., 2017; Li et al., 2018; Wurtzel et al., 2018; Scroxton et al., 2023). We also added a speleothem record from Borneo as an outgroup sample (Chen et al., 2016). The speleothem records used are mostly interpreted as proxies for summer monsoon rainfall changes through regional circulation changes, regional and local rainfall amount (Supplementary Discussion 1).

We conducted three different analyses on different subsets of the ten hydroclimate records. The first analysis (PCA-5Stal) uses the five continuous speleothem records from Oman, India, Sumatra, Rodrigues and Borneo (Figs. 1 and 2, Table 1). The second analysis (PCA-7stal) uses those five speleothems and adds two additional records with brief hiatuses (Australia, Madagascar; Supplementary Discussion 2). Both analyses were run at 15 year resolution. To increase data density around the Indus valley the third analysis (PCA-All) included all seven speleothem records, plus three high resolution, annually laminated, marine cores with proxies interpreted as responding to terrestrial hydroclimate variability. (Deplazes et al., 2013; Giesche et al., 2019). PCA-All was conducted at 20-year resolution to accommodate the lower sampling resolution of the marine sediment cores.

On each suite of high resolution, precisely-dated regional hydroclimate records, we conducted Monte-Carlo principal component analysis (MC-PCA) (Deininger et al., 2017) based on Anchukaitis and Tierney (2012). For the MC-PCA, 2000 age models are created by allowing ages to vary within 1 standard deviation assuming a Gaussian distribution and then linearly interpolating between ages (Supplementary Fig. 1). This creates age models with different temporal resolutions based on the sample spacing. The age models are upscaled to 15 (PCA-5Stal, PCA-7Stal) or 20 (PCA-All) year-long bins using a Gaussian kernel applied to all data points within the bin. Climate records are normalized to mean 0 and standard deviation 1. Principal component analysis (PCA) is then conducted on 2000 sets of upscaled normalized proxy records. Age uncertainties can result in bimodal distributions of principal component (PC) time series. A flipping procedure is used to reinvert the flipped PCs. The final PCA time series is calculated using the mean and standard deviation for each bin. The Kolmogorov-Smirnov (KS) test is used to ensure that only statistically meaningful (95% level) principal components are analyzed. The timing and age uncertainty of specific transitions can be determined from the 2000 principal component simulations of each PCA run.

To detect and quantify the uncertainty on changepoints in PC1 we used RAMPFIT (Mudelsee, 2000, 2013), a Fortran program that

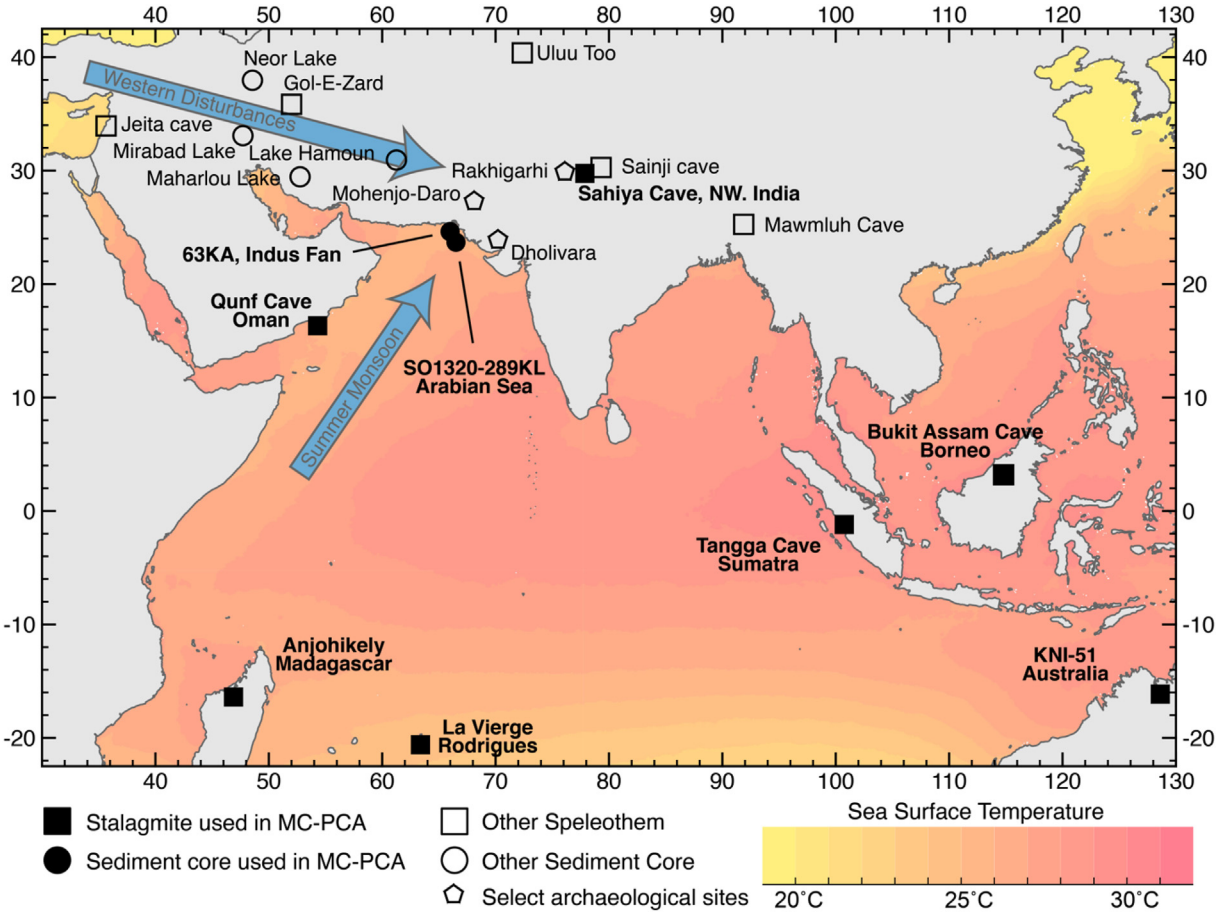

Fig. 1. Location map. Squares denote stalagmite/speleothem paleoclimate sites; circles denote marine sediment cores. Closed symbols are records used in the MC-PCA, open symbols did not pass our MC-PCA quality control criteria. Pentagons indicate location of select Harappan archaeological sites. Color axis for oceans shows modern mean annual sea surface temperature (Basher et al., 2014; Feldman and McClain, 2010). Land shown in grey. Map was created using QGIS 3.8. (For interpretation of the references to color in this figure legend, the reader is referred to the Web version of this article.)

estimates change-points using a weighted least squares regression for the proxy value, a brute force search for the time value, and 10,000 repetitions of a moving block bootstrap to estimate uncertainty. We constrained the search to find both changepoints between 3.1 and 4.5 kyr BP.

3. Results

The dominant mode of variability in Indian Ocean hydroclimate between 5.0 and 3.0 kyr BP is a unidirectional shift between 4.0 and 3.6 kyr BP (Fig. 3a, all lines). RAMPFIT quantifies this shift on PCA-7Stal as starting at 3.97 kyr BP (±80 yr standard error) and ending at 3.76 kyr BP (±70 yr standard error) (Fig. 3c). All three MC-PCA runs produce similar results, indicating that the results are not unduly influenced by which records were selected (Supplementary Discussion 3, Supplementary Table 1). Partial amelioration towards mean conditions occurs between 3.55 and 3.3 kyr but the amelioration is incomplete, suggesting a permanent or semi-permanent (at least to 3 kyr BP) change in regional hydroclimate.

Most individual records load negatively on PC1, indicating that this change was a basin-wide transition from wetter to drier conditions (Fig. 4). A positive loading (i.e., drier to wetter conditions) occurs in the Borneo speleothem record located in the Indo-Pacific Warm Pool. Opposite responses over Borneo and the Indian Ocean may be indicative of atmospheric Walker Circulation changes (Fig. 5a). This could be low-frequency cross-basin coherent changes equivalent to Indian Ocean Basin Mode or Interdecadal Indian Ocean Basin Mode (Huang et al., 2019) or cross-basin dipole changes equivalent to ENSO or the Indian Ocean Dipole (Abram et al., 2007). This suggests zonal climatic processes may dominate over meridional processes in this low frequency variability. Our data supports the idea of a tropical climate shift around 4.0 kyr BP related to zonal climate variability, and provides new constraints on its timing (Denniston et al., 2013; Dutt et al., 2018; Prasad et al., 2014; Toth and Aronson, 2019).

PC2 shows divergent results for different MC-PCA runs. Both the shape (Fig. 3b) and loadings change with the addition of more datasets (Fig. 4). For PCA-5Stal and PCA-7Stal, PC2 positively loading records have drier conditions between 5.0 and 4.9, 4.5 to 3.7 and 3.2 to 3.1 kyr BP and wetter conditions 4.9 to 4.5 and 3.7 to 3.2 kyr BP (green and blue lines). The timing and duration of the 4.5 to 3.7 dry period does not convincingly match the abrupt 4.2 ka event and it also does not appear to be of unusual magnitude. For PCA-All with the additional three sediment cores, PC2 has a much more pronounced and shorter dry period between 4.3 and 3.9 kyr BP (orange line). This result does match the timing and duration of the 4.2 ka event as seen in the Gol-E-Zard Mg/Ca record (Fig. 2b). Therefore, our results confirm a local signal of the 4.2 ka event in the Indus valley. However, the Indian Summer Monsoon records from Oman and NW India do not load in the same direction as the marine sediment core records offshore of the Indus valley. This suggests the 4.2 ka event may not be a coherent feature of the Indian Summer Monsoon.

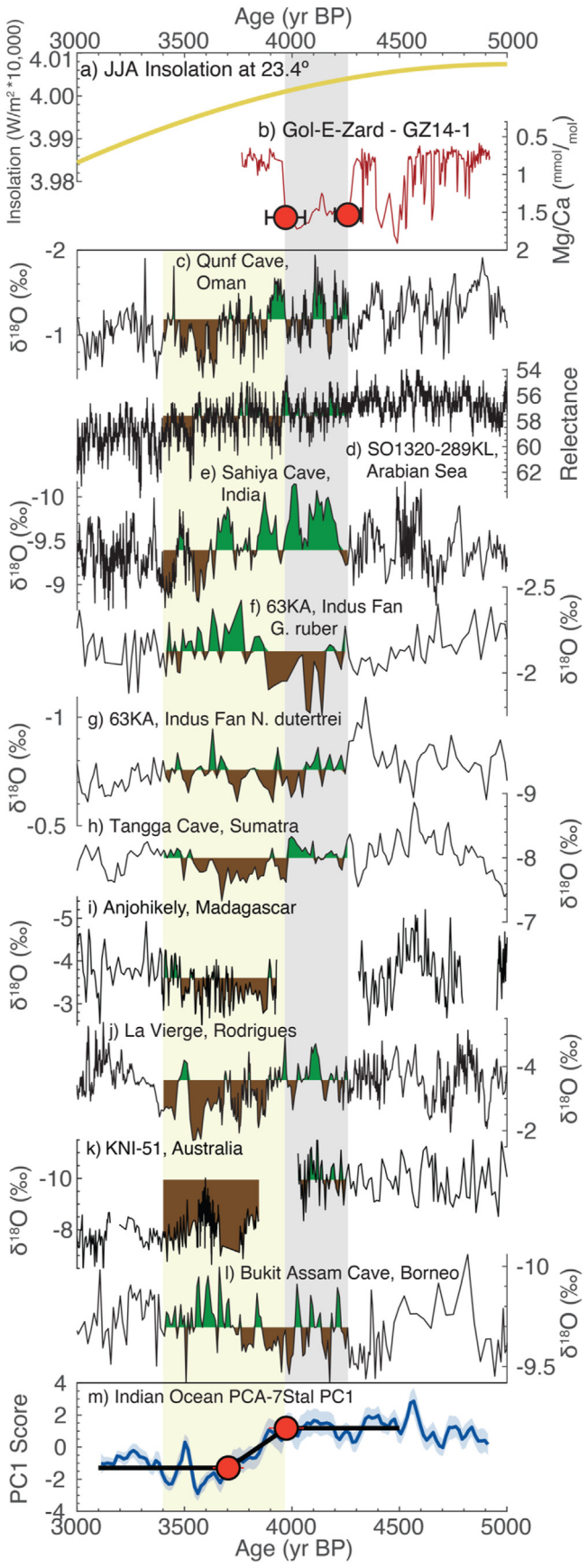

Fig. 2. Comparison of original climate records used in the MC-PCA. a) sum of June/July/August Insolation at the Tropic of Cancer, indicative of northern Hemisphere tropical summer insolation. b) Speleothem Mg/Ca record from Gol-E-Zard, Iran which provides precise timing of the 4.2 ka event. Original tropical Indian Ocean basin hydroclimate records from 5000-3000 yr BP used in Monte-Carlo principal component analysis. c) Q5, Qunf Cave, Oman; d) SO1320-289 KL, Arabian Sea; e) SAH-2, Sahiya Cave, NW India; f) G. ruber, 63 KA, Indus fan; g) N. dutertrei, 63 KA, Indus fan; h) TA12-2, Tangga Cave, Sumatra; i) AK1, Anjohikely, Madagascar; j) LAVI4, La Vierge, Rodrigues; k) KNI-51 composite, Australia; l) BA03, Bukit Assam Cave, Borneo. Green and brown shading indicate values corresponding to conditions that were wetter or drier than the mean values for the records between 5000 and 3000 yrs BP within the shaded boxes. m) Indian Ocean PCA-7Stal with change point that defines the beginning of the tropical dry shift. Grey box indicates the timing of the 4.2 ka event (4.26 to 3.97 kyr BP) as defined at Gol-E-Zard. Yellow box indicates the dry shift from PC1: 3.97-3.4 kyr BP (start defined by the PCA-7Stal PC1 change point).

4. Discussion

The absence of an abrupt onset, 300-year duration, hydroclimate anomaly between 4.26 and 3.97 kyr BP in either the PC1 of all three MC-PCA analysis or PC2 of the PCA-5Stal and PCA-7Stal suggests no significant, widespread 4.2 ka event in tropical Indian Ocean summer hydroclimate. However, such an anomaly is seen in PC2 of PCA-All, i.e., once paleoclimate records derived from Indus valley runoff are included. This suggests some local signal of the 4.2 ka event is observed in the Indus valley. However, as an abrupt event is not seen in the speleothem $\delta^{18}O$ records from Qunf Cave in Oman and Sahiya Cave in northwest India, which are interpreted as proxies for Indian Summer Monsoon variability, the 4.2 ka event may not be a summer monsoon signal, and climate processes other than the 4.2 ka event also influenced hydroclimate variability in the Indus valley during the Mid- to Late-Holocene transition.

In this discussion, we review the paleoclimate signals seen in and around the Indus valley (Section 4.1), investigate regional drivers of past climate in the source areas of both Indus valley summer (Section 4.2) and winter rainfall (Section 4.3), and propose a new chronology of seasonal hydroclimate influencing the Indus valley called the 'Double Drying hypothesis' (Section 4.4). We then explore the consequences of the Double Drying hypothesis for interpretation of changes in the Harappan civilization (Section 4.5) and the location of the GSSP golden spike (Section 4.6).

4.1. Paleoclimate records on the indian subcontinent

Paleoclimate evidence for drying on the subcontinent between 5 and 3 kyr BP falls into three, non-mutually exclusive temporal patterns. Pattern 1 is a long-term unidirectional drying over the entire 5 to 3 kyr period. Pattern 2 is a gradual drying from 4.0 to 3.6 kyr BP. Pattern 3 is a 300-year long dry excursion beginning around 4.25 kyr BP, with return to wet conditions.

Examples of pattern 1 are widespread across the Indian subcontinent (see (Fleitmann et al., 2007)) and include a gradual change in temperature and rainfall between 4.8 and 3.0 kyr BP at PT Tso Lake (Mehrotra et al., 2018), gradual increases in speleothem $\delta^{18}O$ in Yemen, Oman (Fleitmann et al., 2003, 2007), and Mawmluh Cave (Kathayat et al., 2017), and an increase in reflectance in Arabian Sea sediments (Deplazes et al., 2013).

Pattern 2 is a gradual drying from 4.0 to 3.6 kyr BP. It is typically associated with wet conditions between 4.5 and 4.0 kyr BP and sometimes a partial recovery from 3.6 to 3.0 kyr BP (Gupta et al., 2021). It is observed in the Sahiya Cave speleothem $\delta^{18}O$ record (Kathayat et al., 2017), the *Neogloboquadrina dutertrei* $\delta^{18}O$ record from the Indus fan (Giesche et al., 2019), and the speleothem $\delta^{18}O$ records of stalagmites ML.1 and ML.2 from Mawmluh cave (Kathayat et al., 2018). Expressions of Pattern 2 in lower resolution or short paleoclimate records include abrupt drying at paleolake Kotla Dahar at 4.1 kyr BP as recorded in ostracod $\delta^{18}O$ (Dixit et al.,

Table 1
Summary of sites used in Monte-Carlo Principal Component Analysis.

Site	Location	Record	Lat	Lon	Archive	Proxy	Coverage (yr BP)	Res[a]	Data	doi
Qunf Cave	Oman	Q5	17.17	54.30	Speleothem	$\delta^{18}O$	10,558 to 2700	4	351[b]	10.1016/j.quascirev. 2006.04.012
Sahiya Cave	India	SA	30.60	77.87	Speleothem	$\delta^{18}O$	5706 to −56	2	478[b]	10.1126/sciadv.1,701,296
Tangga Cave	Sumatra	TA12-2	−0.35	100.75	Speleothem	$\delta^{18}O$	16,571 to 159	14	436[b]	10.1016/j.epsl. 2018.04.001
Anjohikely	Madagascar	AK1	−15.56	46.88	Speleothem	$\delta^{18}O$	5224 to 1998	5	[c]	10.1016/j.quascirev.2022.107874
La Vierge	Rodrigues	LAVI4	−19.76	63.37	Speleothem	$\delta^{18}O$	6014 to 2999	3	369[b]	10.5194/cp-14-1881-2018
KNI-51	Australia	composite	−15.30	128.62	Speleothem	$\delta^{18}O$	8844 to −58	6	155[d]	10.1016/j.quascirev. 2013.08.004
Bukit Assam Cave	Borneo	BA03	4.03	114.80	Speleothem	$\delta^{18}O$	13,548 to −45	11	238[b]	10.1016/j.epsl. 2016.02.050
63 KA	Indus fan	*G. ruber*	24.62	65.98	Sediment core	$\delta^{18}O$	5413 to 2998	18	[e]	10.5194/cp-15-73-2019
63 KA	Indus fan	*N. dutertrei*	24.62	65.98	Sediment core	$\delta^{18}O$	5413 to 2998	18	[e]	10.5194/cp-15-73-2019
SO130-289 KL	Arabian Sea		23.68	66.50	Sediment core	Reflectance	79,471 to 1789	<1	815,851[f]	10.1038/ngeo1712

[a] Mean resolution between 5000 and 3000 years BP.
[b] SISAL Entity ID.
[c] Data available at: https://www.ncdc.noaa.gov/paleo/study/37062, and submitted to the SISAL database for future release.
[d] SISAL Site ID.
[e] Data available at http://eprints.esc.cam.ac.uk/4371/.
[f] Pangaea Database.

2014), although we recognise that permanent changes in lake dynamics do not necessarily represent permanent changes in hydroclimate. Wet conditions at Surinsar Lake occurred between 4.4 and 4.0 kyr BP (Trivedi and Chauhan, 2009). While likely also influenced by westerlies, the Puruogangri ice cap is interpreted as a tropical record (Thompson et al., 2006). Ice cap $\delta^{18}O$ shows a decrease starting at 4.0 kyr BP with partial recovery at 3.4 kyr BP. The Didwana salt lake became ephemeral around 4.0 kyr BP (Singh et al., 1990). Gradual drying is recorded in peat bog pollen from Garhwal between 4.0 and 3.5 (Phadtare, 2000), and in speleothem $\delta^{18}O$ from Sainji Cave between 4.0 and 3.5 kyr BP (Kotlia et al., 2015). The paleolake Karsandi record shows wet conditions from 5.1 to 4.4 kyr BP, followed by drying (Dixit et al., 2018). The length of drying is unknown due to an undated massive gypsum layer, but there is partial recovery prior to 3.2 kyr BP. A stalagmite from Dharamjali Cave in the Himalaya shows a gradual drying trend between 3.7 and 3.2 kyr BP (Kotlia et al., 2018). Similar changes are also observed in peninsular India, where a period of wet conditions followed by dry conditions between 4.5 and 3.3 kyr BP is observed in the pollen record from Shantisagara Lake (Sandeep et al., 2017).

Pattern 3 is 300-year long dry excursion beginning around 4.25 kyr BP, with return to wet conditions. Paleoclimate records showing Pattern 3 include high resolution records such as the foraminiferal *Globigerinoides ruber* $\delta^{18}O$ record (Giesche et al., 2019; Staubwasser et al., 2003) from the Indus fan, and the KM-A speleothem record from Mawmluh Cave (Berkelhammer et al., 2012). Lower resolution records include lithology, pollen, biomarkers and trace elements from Lonar Lake which suggest a dry period from 4.6 to 3.9 kyr BP, peaking at 4.2 to 4.0 kyr BP, with wet conditions continuing until 3.7 kyr BP (Prasad et al., 2014).

The three patterns are not mutually exclusive. Many paleoclimate records show evidence of more than one pattern. The Lake Rara Mn/Ti record shows a weak monsoon starting early at 4.7 and a partial recovery at 3.5 kyr BP (Nakamura et al., 2016). Similarly, the Lake Agung Co carbonate $\delta^{18}O$ shows a gradual drying trend, but with termination of sediment deposition at 3.9 kyr BP (Morrill et al., 2006). Meanwhile the Al/Ca record of Tso Moriri shows wetter conditions from 5.32 to 4.35 kyr BP, followed by a dry excursion that lasts until 3.4 kyr BP (Dutt et al., 2018). The multi-proxy Tso Kar lake record shows a unidirectional drying transition starting around 4.8 kyr BP, with driest conditions around 4.2 kyr BP (Wünnemann et al., 2010). Stalagmite from TM-18 Tianmen Cave stops growing at 4.15 kyr BP (±180 years) (Cai et al., 2012), potentially consistent with any or all three drying signals.

All these paleoclimate records are proxies for parts of the hydroclimate system. However, they cannot all be recording basin-scale variability in the summer monsoon. Instead, different proxy systems might record local effects, have variable system memory, be affected by changing temperatures, evaporation rates and cloud cover differently, or show sensitivity to different seasons. To elucidate which pattern might correspond to which season or climatic control, we compare the three Indian subcontinent hydroclimate patterns with wider regional hydroclimate.

4.2. Mid- to Late-Holocene climate change in the source region of Indian Summer Monsoon rainfall

Pattern 1 is a gradual drying between 5 and 3 kyr BP (type example: Fig. 2a). It is likely part of the gradual reduction in northern hemisphere tropical and subtropical rainfall over the course of the Holocene (Haug et al., 2001; Schneider et al., 2014). This underlying secular trend in Holocene climate is caused by decreasing summer insolation from changing orbital precession. In the Indian Summer Monsoon domain this trend is clearly expressed in full Holocene length speleothem records from Oman (Fleitmann et al., 2003) and Mawmluh Cave (Berkelhammer et al., 2012). A gradual trend in forcing can lead to threshold changes in climate due to feedbacks in the climate system, e.g., the termination of the Green Sahara Period (Tierney and deMenocal, 2013). Therefore, unidirectional drying events on the Indian subcontinent throughout the Holocene may be due to threshold effects and local feedbacks on this secular trend.

Pattern 2 is a drying trend from ~4.0 to 3.6 kyr BP (type example: Fig. 2b, yellow shading in Fig. 2). It matches the PC1 of all three tropical Indian Ocean basin hydroclimate PCA. As our PCA focuses only on the highest resolution, most precisely dated records available, it is dominated by speleothem records. Speleothem carbonate $\delta^{18}O$ tends to record amounted-weighted changes in precipitation $\delta^{18}O$. As a result, they are likely biased towards local summer monsoonal rainfall. A shift in tropical hydroclimate beginning around 4 kyr BP is widely recognised in other Indian Ocean tropical hydroclimate records (de Boer et al., 2014; Denniston et al., 2013; Gagan et al., 2004; Giosan et al., 2018; Li et al., 2018; MacDonald, 2011; Toth et al., 2012). The inferred mechanism is an abrupt change in El Niño-Southern Oscillation (ENSO) behavior around 4.0 kyr BP with an increase in the frequency or magnitude of El Niño events (de Boer et al., 2014; Denniston et al., 2013; Gagan et al., 2004; MacDonald, 2011; Toth et al., 2012), and/or a narrowing of the tropical rainbelt (Li et al., 2018). In the modern climate system, El Niño events are associated with reduced Indian summer monsoon precipitation (Mooley and Parthasarathy, 1983). Therefore, an increase in the frequency

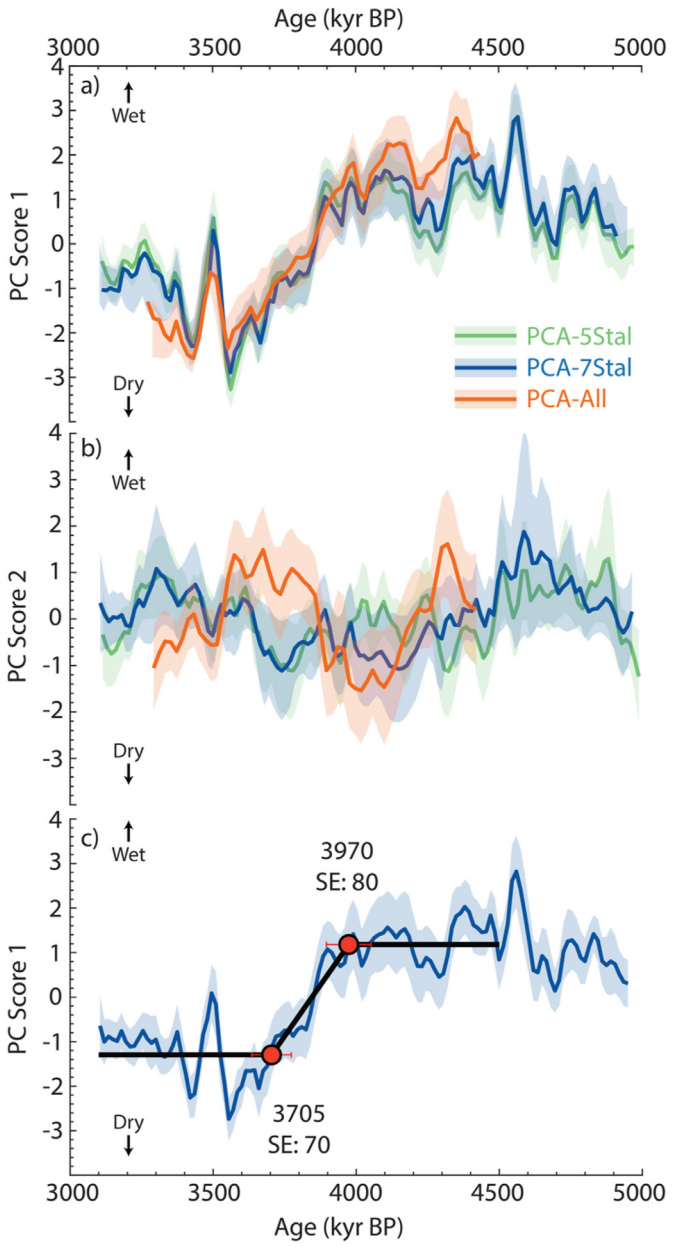

Fig. 3. Monte-Carlo Principal component analysis of tropical Indian Ocean hydroclimate records: a) Principal Component 1, b) Principal Component 2. Color lines indicate mean principal component from 2000 individual analyses on redrawn age models, with 1 standard deviation shading. c) RAMPFIT results of PCA-7Stal, PC1 (black line with red circles and red error bars on ramp start and end points). Green: Five speleothem PCA, Blue: 7 speleothem PCA, Orange: 7 speleothem and 3 sediment core PCA.

and/or magnitude of El Niño events would be expected to cause a decrease in time-averaged precipitation in the Indus valley. Overall, we interpret Pattern 2 as the dominant signal of Indian Ocean hydroclimate variability at the Mid-to Late-Holocene transition, and therefore likely the dominant control on Indian Summer Monsoon variability.

4.3. Mid- to Late-Holocene climate change in the source region of Indus valley winter rainfall

Pattern 3 is an abrupt drying beginning around 4.25 kyr BP, lasting for approximately 300 years with a return to wet conditions afterwards (type example: Fig. 2m, grey shading in Fig. 2). Pattern 3 is observed in PCA-All PC2 but not in PCA-5Stal PC2 or PCA-7Stal PC2, i.e., it only becomes a feature of our analysis once the offshore Indus valley sediment core records are included in our analysis. The spatial dipole of this signal (Fig. 5b) has positive loading (drier conditions between 4.2 and 3.9 kyr) in the three offshore Indus valley records, and negative loading (wetter conditions between 4.2 and 3.9 kyr BP) through most of the rest of the Indian Ocean records. This opposite loading includes the Oman and NW India stalagmite records, which are interpreted as proxies for variability in Indian Summer Monsoon strength via cross Arabian Sea wind strength and integrated moisture rainout respectively (Fleitmann et al., 2007; Kathayat et al., 2017). This suggests that Pattern 3 does not represent Indian Ocean hydroclimate variability, and by extension may not represent Indian Summer Monsoon variability.

Instead, Pattern 3 matches the expression of the 4.2 ka event in the Mediterranean and Middle East (Fig. 6). In the Middle East the 4.2 ka event is likely manifested as a reduction in winter rainfall. This is intuitive given that precipitation is concentrated in winter months (DJF) (Enzel et al., 2003). Specific seasonally resolved or seasonally sensitive evidence for a reduction in winter rainfall in the region includes a pollen record from Tell Tweini (Kaniewski et al., 2008), a coral record from the Gulf of Oman indicating increased winter shamals and dust storms (Watanabe et al., 2019), and a positive $\delta^{18}O$ excursion in speleothems from Gol-E-Zard (Carolin et al., 2019). In the modern negative $\delta^{18}O_{precip}$ occurs in Iran during winter months (Carolin et al., 2019; Mehterian et al., 2017).

Winter rainfall over the Middle East is largely sourced from the eastern Mediterranean. The synoptic weather systems continue eastwards in the form of Western Disturbances, with additional moisture from the Caspian and Arabian Seas. Western Disturbances are upper tropospheric cyclonic storms carried by the Subtropical Westerly Jet (Dimri et al., 2015; Midhuna et al., 2020) and references within both), moving across Iran and Afghanistan into.

Pakistan and India until they reach the blocking Karakoram and western Himalaya. Western disturbances are the major source of winter rainfall in Pakistan, the Indus valley and north-west India, and winter snowfall in the western Himalayas (Cannon et al., 2015; Lang and Barros, 2004; Midhuna et al., 2020). They provide important moisture sources for growing the winter 'rabi' crops, snowpack, and subsequent spring flow of the Indus (Yadav et al., 2012).

At present, winter rainfall in the Indus valley is only a very small proportion of total annual rainfall (Fig. 7). However, recent studies have proposed an increase in winter rainfall at 4.5 kyr BP (Giesche et al., 2019; Giosan et al., 2018), which suggests potential for winter rainfall to play an important role in annual rainfall budgets, and influence paleoclimate records. Giesche et al. (2019) proposed that the 4.2 ka event drying in the Indus valley was partly caused by a reduction in winter rainfall, potentially sharing the same climate mechanism as drying in the Middle East. Could the 4.2 ka event have propagated into the Indus valley via a decrease in winter rainfall?

Evidence from paleoclimate records on the Western disturbance pathway through Iran, Iraq, Afghanistan, and Pakistan suggest this is a plausible hypothesis. While insufficient high-resolution records yet exist for us to provide a comparable analysis to the Indian Ocean synthesis (Burstyn et al., 2019), available high-resolution records do tend to show a dry event beginning at 4.2 kyr BP while lower resolution records show a mixed response. In Fig. 8 we detail the progression from west to east. The Mediterranean response is shown first by the stalagmites from Buca della Renella in Italy

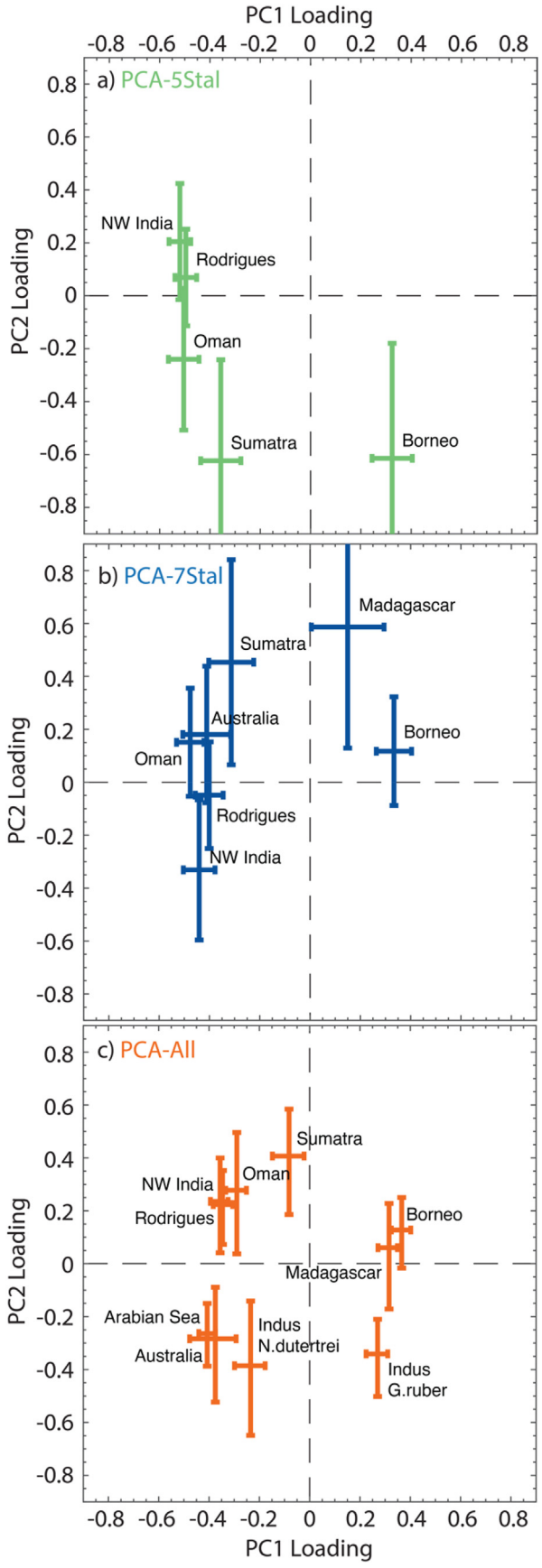

Fig. 4. Loadings of individual hydroclimate records on the first two principal components for each MC-PCA analysis with 1 standard deviation error bars. a) PCA-5Stal, b) PCA-7Stal, c) PCA-All.

(Zanchetta, G et al., 2016; Isola et al., 2019), using a 2018 updated chronology available in the SISAL database (Atsawawaranunt et al., 2018)) and Jeita cave in Lebanon (see Bini et al. (2019)) for full Mediterranean data synthesis). Then from west to east across the Middle East, the current evidence includes a multi-proxy record from Mirabad Lake in Iran (33.08°N 47.71°E) which shows no severe drying (Stevens et al., 2006), but may not have the sampling resolution to see such an event. The Neor Lake (37.96°N, 48.55°E) record of aeolian input and hydrological conditions shows drying and dustiness in two events from 4.24 to 4.14 and 4.04 to 3.97 kyr BP, but relatively wet conditions in-between (Sharifi et al., 2015). The Gol-E-Zard speleothem $\delta^{18}O$ records (35.84°N, 52.00°E) (Carolin et al., 2019) indicates a reduction in winter rainfall. Pollen analysis from Maharlou Lake (~29.45°N, 52.75°E) suggests no major upheaval at the Mid-to Late-Holocene transition, with continuous human cultivation (Djamali et al., 2009). A lake sediment magnetic susceptibility record from Lake Hamoun in Iran (30.93°N, 61.25°E) suggests some transient dry event around the Mid-to Late-Holocene, but the dating is insufficient to confirm a 4.2 kyr BP timing (Hamzeh et al., 2016). In the Indus valley itself, carbon isotope values of rice grains, a summer crop, show increased drying only after 4.0 kyr BP in both Gujarat and Indus valley locations, indicative of no substantial change to summer rainfall between 4.2 and 3.9 kyr BP (Kaushal et al., 2019) .

A wet episode between 4.3 and 4.1 kyr BP, followed by dry conditions between 4.1 and 4.0 kyr BP, occurs in the likely winter westerly dominated Uluu-2 speleothem record from Uluu-Too cave in Kyrgyzstan (40.38°N, 72.35°E) (Wolff et al., 2017). The two opposing signals prevent further determination of the climatic mechanism driving this record at this time. A latitudinal change in winter westerlies, consistent with reduced Western Disturbances might be expected to cause a wet anomaly at Uluu-Too, whereas an overall reduction in moisture transport from the Mediterranean might be expected to cause a dry anomaly.

Therefore it is plausible that at the 4.2 ka event, weakened or reduced Western Disturbances originating in the Mediterranean and travelling along a southern route over Iraq, Afghanistan and Pakistan to the Indus valley led to reduced eastward moisture transport and winter rainfall (Dimri et al., 2015; Syed et al., 2006). The exact climate driver of a change in Western Disturbances remains unclear. While a negative excursion of the North Atlantic Oscillation close to 4.2 kyr BP (Olsen et al., 2012) would cause a reduction in rainfall from Western Disturbances (Syed et al., 2006), the pattern of Mediterranean climate anomalies suggests a more complex set of drivers than a simple North Atlantic Oscillation excursion influencing winter rainfall (Bini et al., 2019; Kaniewski et al., 2018).

Indeed, the combined evidence is for an absence of the 4.2 ka event in tropical Indian Ocean records reflecting monsoon rainfall, especially the Indian Summer monsoon records from Oman and NW India (section 4.1, Figs. 4b, Fig. 5b), and a 4.2 ka event that propagated through the Middle East via Western Disturbances during boreal winter (section 4.2, Fig. 7c). Therefore, we propose that the 300-year long drying in the Indus valley at the Mid- to Late-Holocene transition, commencing at 4.26 kyr BP (i.e. Pattern 3), is mostly, or even wholly, a winter rainfall drying.

4.4. The Double Drying hypothesis

Taking into account evidence of hydroclimate variability in the source areas of both summer and winter rainfall in the Indus valley, we propose the 'Double Drying hypothesis' to describe and explain rainfall variability in the Indus valley at the Mid- to Late-Holocene transition. An abrupt decline in winter rainfall from 4.26 to 3.97 was immediately followed by a more gradual but larger and longer-

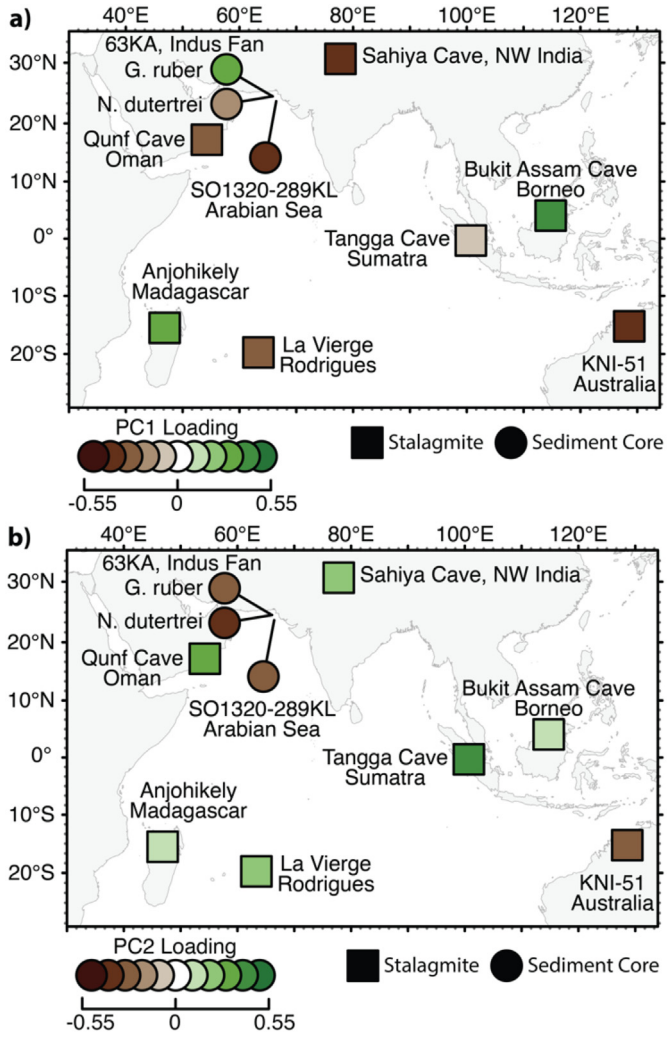

Fig. 5. Spatial variability of loadings of individual hydroclimate records on PCA-All. *a) PC1, b) PC2.*

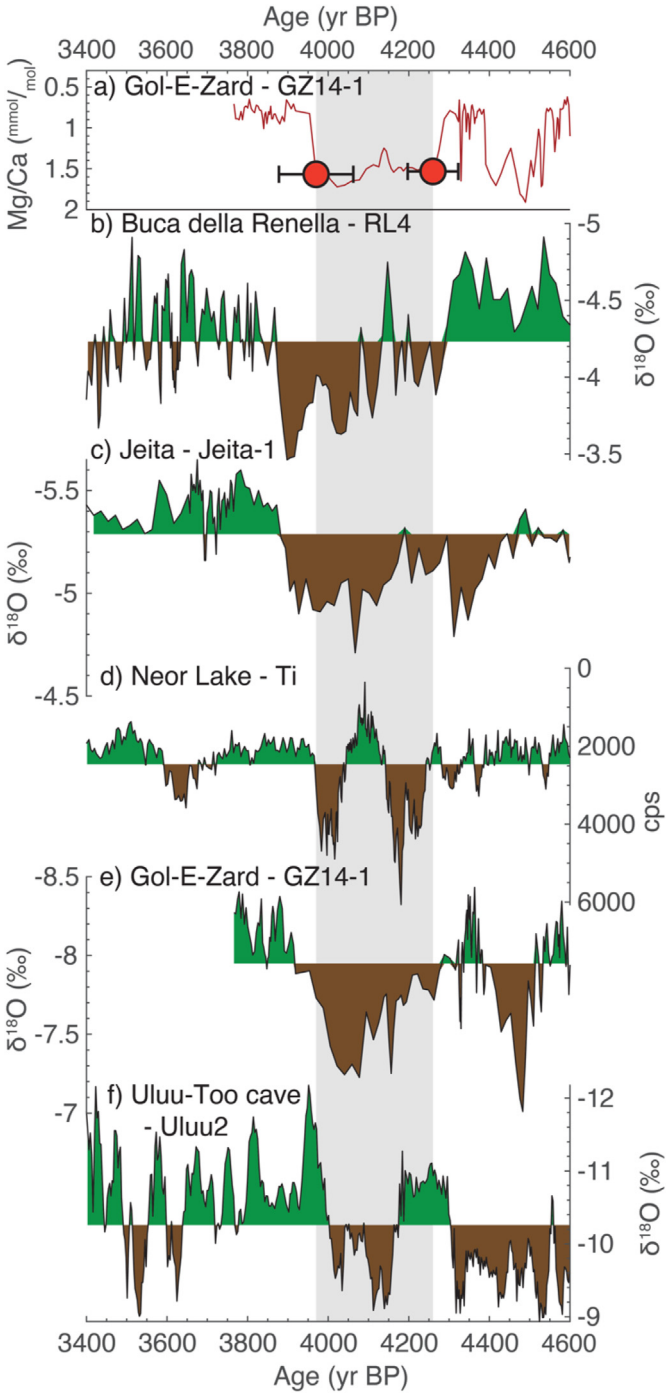

Fig. 6. Individual hydroclimate records along a west to east transect from the Mediterranean through the Middle East along the Western Disturbances route. a) Speleothem Mg/Ca record from Gol-E-Zard, Iran which provides precise timing of the 4.2 ka *event; b) Speleothem RL4, Buca della Renella* cave, *Italy; c) Speleothem Jeita-1, Jeita* cave, *Lebanon; d) Neor Lake sediment core Ti counts, Iran; e) Speleothem GZ14-1, Gol-E-Zard, Iran; f) Speleothem Uluu2, Uluu-Too* cave, *Kyrgyzstan. Grey box indicates the 4.2* ka *event as determined in* Carolin et al. *(2019) (4.26–3.97 kyr BP) (Pattern 3).*

lasting decline in summer rainfall. The winter rainfall decline was abrupt, likely caused by a reduced precipitation from Westerly Disturbances, and is linked to the 4.2 ka event. Summer monsoon drying occurred more gradually between 3.97 and 3.70 kyr BP (estimated from RAMPFIT of PCA-7Stal PC1), and the drying lasted for several centuries, in some areas being a permanent change in rainfall. The summer monsoon drying was likely the response to a shift in the mean state of tropical zonal circulation, and possibly an increase in El Niño frequency. Both dryings occur on an underlying secular trend of decreasing northern hemisphere tropical summer rainfall over the course of the Holocene, driven by decreasing insolation.

The Double Drying hypothesis is not entirely new. Leipe et al. (2014)previously suggested two reductions in precipitation around 4.4 and 4.0 kyr BP based on evidence from the Tso Moriri pollen record. The first drying was interpreted as being associated with North-Atlantic variability via changes in mid-latitude westerlies, and the second drying was interpreted as resulting from changes in monsoonal rainfall, with changing ENSO variability as a potential mechanism. The Double Drying hypothesis builds on the Leipe et al. hypothesis, adding a regional framework and the enhanced chronology of U–Th dated stalagmites. However, we do not find evidence for slightly wetter conditions between these two events.

The Double Drying hypothesis also builds on recent high resolution paleoclimate work in the region. Both Giosan et al. (2018) and Giesche et al. (2019) proposed an increase in winter rainfall at 4.5 kyr BP. However, Giesche et al. (2019) suggested a winter rainfall drying starting around 4.3 kyr BP and peaking at 4.1 kyr BP, whereas Giosan et al. (2019) suggested that the period of increased

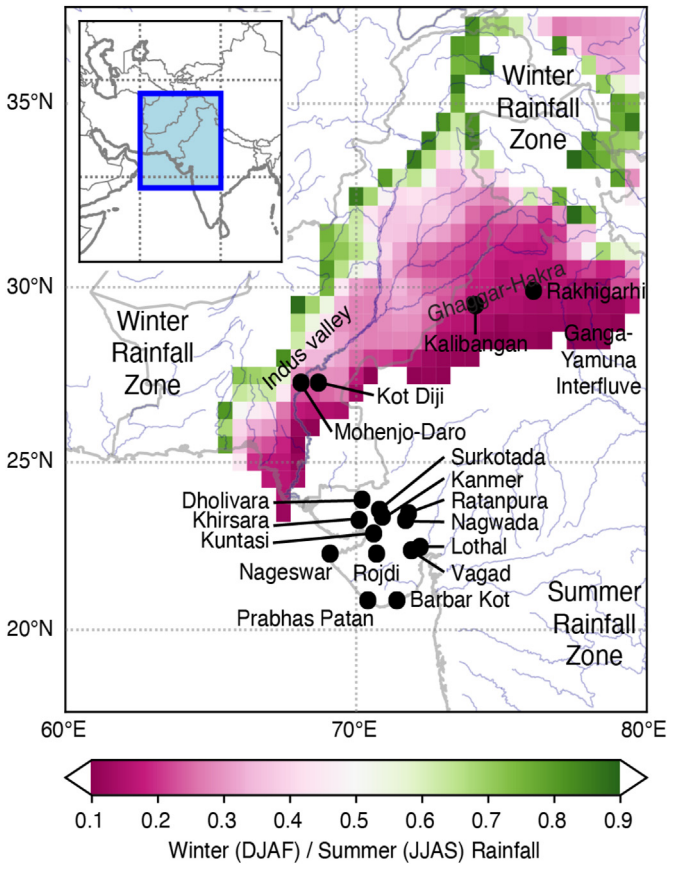

Fig. 7. Location map of Indus valley precipitation seasonality (color axis) and significant archaeological sites (black dots). Color axis (pink to white to green) shows winter (DJAF) season rainfall divided by summer (JJAS) season rainfall, between 1981 and 2010 using Global Precipitation Climatology Centre (GPCC) Full Data Reanalysis Version 7 0.5° × 0.5° Monthly Totals (Schneider et al., 2015). Areas with greater than 90% rainfall falling in summer compared to winter, or vice-versa are left white and labelled.

winter rainfall lasted to 3.0 kyr BP. As our analysis is dominated by speleothem $\delta^{18}O$ records, our PCA may not directly include or infer winter rainfall. However, increases in PCA-5Stal PC2 and PCA-7Stal PC2 between 4.5 and 4.3 kyr BP (Fig. 3) are supportive of increased moisture availability, and the absence of a 4.2 kyr event signal in the likely summer rainfall dominated PC1 agrees with the idea of a winter rainfall drying being the cause. Similarly, the PCA does not allow for firm conclusions about whether winter rainfall increases at 3.9 kyr BP. However, the most likely mechanism for winter drying, a change in Western Disturbances from the Mediterranean related to the 4.2 ka event ended abruptly at 3.9 kyr BP, suggesting a return of abundant winter rainfall that presumably continued to 3.0 kyr BP (Giosan et al., 2019).

Giesche et al. (2019) also proposed a decrease in summer rainfall associated with the 4.2 ka event, as part of a long-term trend since at least 4.8 kyr BP, peaking at 4.2 kyr BP, with a return to pre-excursion values by 3.0 kyr BP. Again, our PCA cannot weigh in on a secular trend of decreasing rainfall. But we feel there is a little doubt that there was a gradual decrease in monsoonal rainfall, likely resulting from decreasing northern hemisphere insolation over the course of the Holocene. Our PC1, and several individual records also agree with at least a partial recovery by 3.0 kyr BP. Our synthesis disagrees with Giesche et al. (2019) on the timing of the summer rainfall drying on top of the secular trend. Giesche et al. (2019) suggest summer drying shortly after 4.2 kyr BP, i.e., a simultaneous drying in both summer and winter rainfall. In contrast, the regional PCA suggests summer drying beginning at 3.97 and peaking at 3.6 kyr BP, i.e., a sequential double drying. As discussed in Giesche et al. (2019) and Section 4.1 above, numerous hydroclimate paleoclimate records from the region support one or more of the three drying patterns: Pattern 1: a secular trend, Pattern 2: a 4.0 kyr BP step change, and Pattern 3: a 4.2–3.9 kyr BP anomaly. To reconcile the exact timing of these rainfall fluctuations and their seasonality, further study is required with paleohydroclimate proxies with less ambiguous seasonality than speleothem and foraminiferal stable isotopes.

Nevertheless, our Double Drying Hypothesis is consistent with broader climatic changes in 'upstream' areas of Indus valley rainfall; changes in winter mid-latitude westerlies are interpreted as influencing winter rainfall, while changes in tropical Indian Ocean hydroclimate are interpreted as influencing summer monsoonal rainfall.

4.5. The Double Drying hypothesis as climatic context for the Harappan civilization

Human societies have lived in the Indus valley for ~9000 years, with societal changes linked to changes in rainfall and fluvial water availability (Gupta et al., 2006). The Harappan civilization began around 5.2 kyr BP (Possehl, 2002), reaching its peak between 4.8 and 3.8 kyr BP, during the Mature Harappan period. Cultural decline, including poor pottery craftsmanship and reduced reservoir maintenance or abandoned water reservoirs, began as early as 4.3 kyr BP (Sengupta et al., 2020) leading into the Late Mature Harappan period with societal reorganization, site abandonment and migration underway before 3.9 kyr BP (Possehl, 2002; Sengupta et al., 2020; Vahia and Yadav, 2011). During the Late Harappan period (3.9–3.0 kyr BP), technological decline, settlement size reductions and abandonment continued (Possehl, 1993, 1997, 2002; Sengupta et al., 2020). By 3.0 kyr BP, Post-Urban Harappan society had become rural with few cultural similarities to the Harappan. Post-Urban Harappan settlements were concentrated around the Ganga-Yamuna interfluve and southern Gujarat, which have higher summer rainfall than the Indus plain (Gangal et al., 2010; Petrie et al., 2017).

An association of the end of the Mature Harappan period and the 4.2 ka event has been widely made in the literature (Berkelhammer et al., 2012; Dixit et al., 2014, 2018; Giosan et al., 2012; Kathayat et al., 2017; Staubwasser et al., 2003). The assumed mechanism is usually a decline in summer monsoonal rainfall. However, the idea has been resisted by many in the archaeological community for several reasons: 1) There is evidence for long-term drying over the course of the Holocene, suggesting that the Mature Harappan developed in response to water stress rather than pluvial conditions (Gupta et al., 2003; Madella and Fuller, 2006). 2) There is evidence for drying, adaptation and continuation within the Mature Harappan (Pokharia et al., 2017). There are also two key climate problems with a summer monsoon mechanism: 1) Evidence for drying in the subcontinent does not typically support an abrupt 300-year long drying with subsequent return to wet conditions, as might be expected if the 4.2 ka event were the cause (Madella and Fuller, 2006; Wright et al., 2008). 2) The most likely climate mechanism of change to the Indian Summer Monsoon, a shift in ENSO state and increased El Niño frequency, occurs well after the beginning of decline (MacDonald, 2011).

While the causes of societal decline and transitions are undoubtably multifaceted and complex, the role of climate in the end of the Mature Harappan requires study. Further, a climate

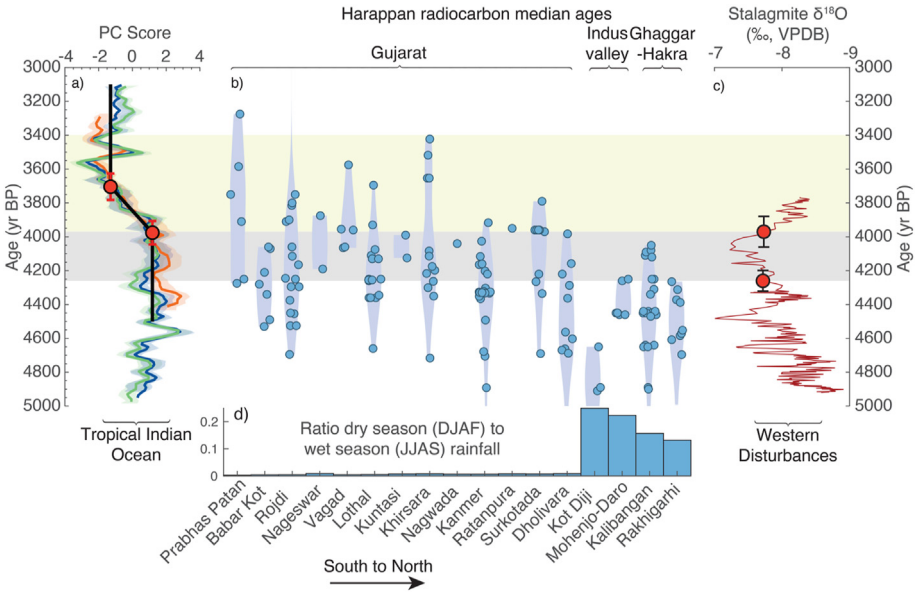

Fig. 8. Climatic changes and the Harappan civilization between 5 and 3 kyr BP. a) results from the Monte-Carlo principal component analysis of Indian Ocean hydroclimate records. PC1 from the 5 speleothem PCA (green) (Pattern 2), 7 speleothem PCA (blue) and 7 speleothems plus 3 sediment core PCA (orange) with 1 standard deviation shading. RAMPFIT results of PCA-7Stal, PC1 (black line with red circles and error bars on ramp start and end points). b) Violin plot of median ages of radiocarbon dates at major Harappan archaeological sites (blue dots) with kernel density estimate (blue shading). Plot adapted from Sengupta et al. (2020) with radiocarbon data from: Kalibangan, Kot Diji, Mohenjo-Daro (Brunswig, 1975), Prabhas Patan, Babar Kot, Nagwada, Surkotada, Raranpura, Kuntasi, Nagwada, Vagad, Lothal, Nageswar (Herman, 1996), Rojdi (Brunswig, 1975; Herman, 1996), Kanmer (Pokharia et al., 2011), Rakhigarhi (Nath et al., 2014; Vahia et al., 2016), Khirsara (Pokharia et al., 2017), Dholivara (Sengupta et al., 2020). c) GZ14-1 δ18O from Gol-E-Zard (Pattern 3). Red circles and black error bars denote start and end of the 4.2 ka event. d) Ratio of mean rainfall (1981–2010, GPCC V7 global gridded dataset at 0.5° × 0.5° resolution (Schneider et al., 2015)) falling in winter (DJAF) vs summer (JJAS) at each archaeological site. Grey box indicates the 4.2 ka event as determined in Carolin et al. (2019) (4.26–3.97 kyr BP) (Pattern 3). Yellow box indicates the 3.97–3.4 kyr drying (Pattern 2).

focused study is unlikely to elucidate further the relative role of climate in societal change, particularly without more precise and detailed chronologies from archaeological sites. The nature, location, and precise timing of societal change in response to the two consecutive dryings are likely due to complex biogeophysical (Cookson et al., 2019), geomorphological (Giosan et al., 2012) and/or social processes and feedbacks (Madella and Fuller, 2006; Petrie et al., 2017; Schug et al., 2013). Nevertheless, the Double Drying hypothesis provides important climatological context for the Harappan civilization.

The Double Drying hypothesis may solve the seasonal cropping paradox. The Harappan grew both winter and summer rainfall crops. During the Late Mature Harappan period, there was a switch in proportions from barley and wheat to millet (Petrie et al., 2017; Petrie and Bates, 2017; Pokharia et al., 2017), particularly at continuing peripheral sites (Pokharia et al., 2014). At present, barley and wheat are winter crops and millet a summer crop (Petrie and Bates, 2017). Therefore, assuming similar copping patterns, the agricultural evidence suggests a switch from winter to summer crops. This is supported by carbon isotopes of rice grains (a summer crop), which show drying only after 4.0 kyr BP, in both Gujarat and the Indus valley (Kaushal et al., 2019). A winter rainfall drying between 4.26 and 3.97 kyr BP, followed by a summer rainfall drying from 3.97 kyr BP provides more a coherent explanation of these changes than a summer rainfall drying between 4.26 and 3.97 kyr BP.

There are some important caveats and nuance, namely 1) there is substantial geographic variation in crops between Harappan sites, 2) winter crops are reliant on residual soil moisture from the summer rains, 3) the Harappan may have engaged in multicropping (multiple crops in the same land at the same time) or strategies not aligned with modern practices and 4) the timing of rainfall and peak river flow/flooding may not be simultaneous owing to upstream snow melt (Petrie and Bates, 2017). Regardless, changing crop patterns demonstrates adaptation strategies by the Harappan to changing seasonality of rainfall.

The Double Drying hypothesis may also fit with the pattern of movement and the timing of urban abandonment (Fig. 8b). At Indus valley sites such as Kot Diji and Mohenjo-Daro, a compilation of radiocarbon ages show no dates beyond 4.25 kyr BP (Sengupta et al., 2020). North-easterly sites in the Ghaggar-Hakra area show either a similar pattern at the major urban centre (Rakhigarhi), some extension towards 3.9 kyr BP (Kalibangan) or post 3.9 kyr BP continuation at more-peripheral sites (Masudpur; Petrie et al., 2016). These later sites are typically Late Harappan (i.e., after the Mature period). In the south, Late Harappan sites in Gujarat also consistently extend beyond 4.0 kyr BP at Prabhas Patan, Rojdi, Nageswar, Vagad, Lothal, Khirsara, Kanmer, Ratanpura and Surkotada (Sengupta et al., 2020).

Next, we compare this temporal-spatial pattern to the modern seasonal rainfall distribution. Under modern climate the proportion of winter rainfall varies greatly across the area of Harappan occupation, from a couple of percent in Gujarat, through to 20% at the Indus valley and Ghaggar-Hakra sites, to greater than 90% on the western boundary of the Harappan civilization in western Pakistan (Figs. 7 and 8d) (MacDonald, 2011). This pattern may have been different during the Mid-Holocene. The Mature Harappan likely coincided with enhanced winter rainfall from increased Western Disturbances (Dixit et al., 2018; Giosan et al., 2018; Singh, 1971; Wright et al., 2008), increasing the winter rainfall totals and percentages.

A 4.26–3.97 kyr BP winter rainfall drying therefore fits with the spatial pattern of abandonment. More winter rainfall dependent sites in the north and west appear (at least within current

radiocarbon constraints) to be abandoned earlier. The summer rainfall drying beginning 3.97 kyr BP is then associated with the gradual abandonment of remaining major Harappan settlements in summer rainfall dominated areas (such as those in Gujarat), and transition to more rural society. The transition to Post-Urban Harappan societies saw migration to two areas: the Ganga-Yamuna interfluve and southern Gujarat. These areas have higher absolute summer rainfall amounts, and therefore could be considered climate refugia in the face of reduced summer monsoonal rainfall in and around the Indus valley.

4.6. Consequences for the Mid- to Late-Holocene GSSP

The Mawmluh Cave speleothem records which define the 4.2 ka event (Berkelhammer et al., 2012; Walker et al., 2018) are too short to be included in our PCA analysis (Fig. 9). However, the highest resolution replicated record from the cave, ML.1, replicated by ML.2, shows gradual drying over its entire growth period, wetter than normal conditions at 4.1–4.0 kyr BP, and a step-change increase in $\delta^{18}O$ at 4.0 kyr BP (Kathayat et al., 2018). These results are consistent with both the secular millennial scale drying trend (Pattern 1), and the 4.0 kyr BP summer monsoon drying identified in PC1 (Pattern 2).

The Global Boundary Stratotype Section and Point (GSSP) golden spike is in stalagmite KM-A from Mawmluh Cave (Berkelhammer et al., 2012). KM-A does not replicate ML.1 or ML.2 from the same cave. Instead, KM-A contains two increases in $\delta^{18}O$ (drying events), one at 4.31 kyr BP and one at 4.05 kyr BP. Within reasonable age uncertainty (±30 years at the nearest U–Th date, so likely slightly higher away from the age) the timing of the KM-A dry anomalies at 4.31 kyr BP and 4.05 kyr BP are consistent either 1) both 4.26 and a 3.97 kyr BP drying events (Pattern 2 and Pattern 3), or 2) with the Gol-E-Zard $\delta^{18}O$ record which shows increases at 4.26 and again at 4.09 kyr BP (Pattern 3 only). Recent work on hydroclimate proxy variability at this site suggest some drip sites are significantly influenced by dry season variability (Ronay et al., 2019). Therefore, KM-A may not be an exclusive record of summer monsoon rainfall but may in fact be partly or mostly a winter rainfall record.

There are also notable issues with the stalagmite itself. While the ages of KM-A are very precise, there are only three ages between 5084 and 3654 yr BP and stalagmite growth is very slow. The shape of the stalagmite after 5 kyr BP is not convincing of unaltered equilibrium deposition. Even if the $\delta^{18}O$ record of KM-A does record both drying events the golden spike location at 4.20 kyr BP is part of a run of 40 consecutive $\delta^{18}O$ samples with relatively minor variability (<1‰) between the two drying events. The existence of the Northgrippian-Meghalayan GSSP golden spike in a record with low dating frequency, not replicable within its own locality, not representative of climate variability across its inferred climatic domain, and ambiguously defined as the mid-point between two different climate events, is problematic at a minimum (Helama and Oinonen, 2019). We recommend that an alternative GSSP golden spike for the Mid-to Late-Holocene transition be identified.

5. Conclusions

We investigated regional paleoclimate records in the 'upstream' source areas of Indus valley rainfall. Regional tropical hydroclimate variability between 5 and 3 kyr BP is dominated by a region-wide drying beginning at 3.97 kyr BP (±80 yr, 1SE), with no regionally coherent abrupt 4.2 ka event. In contrast, there is evidence that the 4.2 ka event was transmitted from the Mediterranean through the Middle East via a reduction in precipitation from Westerly Disturbances. This suggests that the 4.2 ka event influenced winter rainfall in the Indus valley.

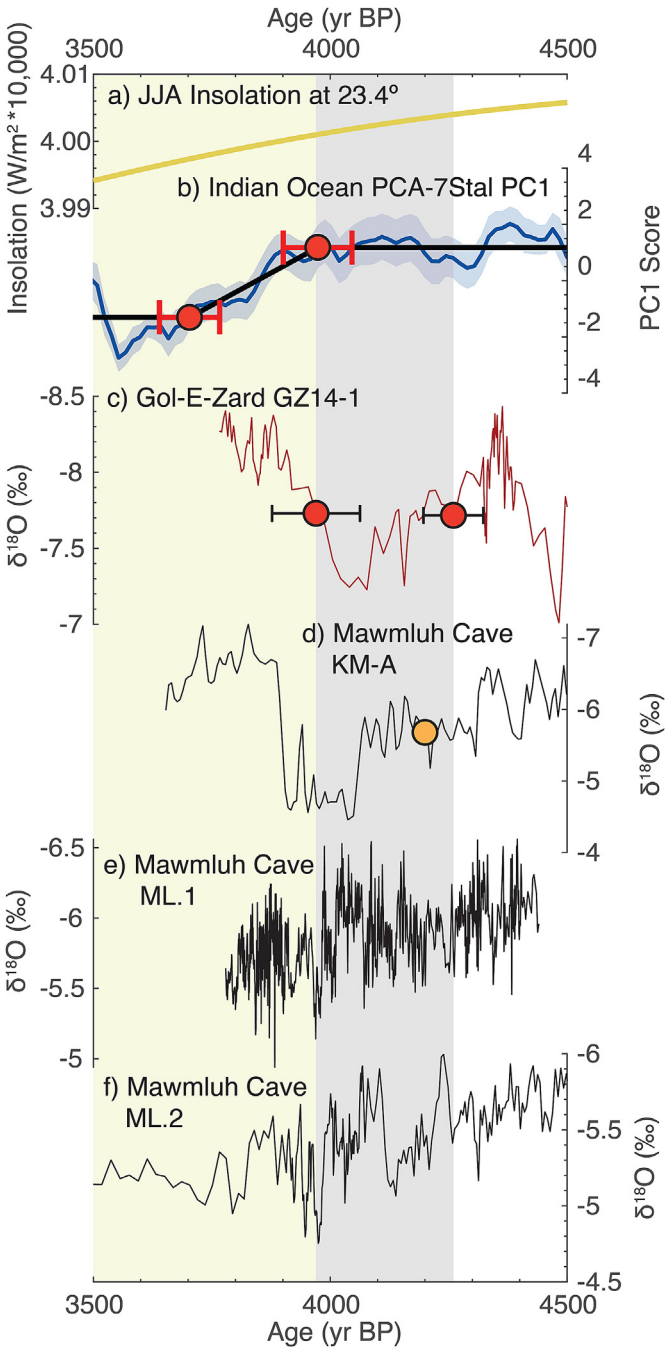

Fig. 9. Comparison of the three climate patterns seen in the Indus valley and the Mawmluh Cave stalagmites from eastern India. a) sum of June/July/August Insolation at the Tropic of Cancer, indicative of northern Hemisphere tropical summer insolation; b) PC1 from the 7 speleothem PCA (blue) (Pattern 2) with RAMPFIT results of PCA-7Stal PC1 (black line with red circles and error bars on ramp start and end points); c) GZ14-1 stalagmite $\delta^{18}O$ from Gol-E-Zard (Pattern 3). Red circles and black error bars denote start and end of the 4.2 ka event; d) Mawmluh Cave KM-A stalagmite $\delta^{18}O$, with gold circle denoting position of the Northgrippian-Meghalayan GSSP golden spike; e) Mawmluh Cave ML.1 stalagmite $\delta^{18}O$; f) Mawmluh Cave ML.2 stalagmite $\delta^{18}O$. Grey box indicates the 4.2 ka event as determined in Carolin et al. (2019) (4.26–3.97 kyr BP). Yellow box indicates the 3.97–3.4 kyr drying. (For interpretation of the references to color in this figure legend, the reader is referred to the Web version of this article.)

We propose the "Double Drying hypothesis" to explain the pattern of rainfall variability in the Indus valley during the Mid- to Late-Holocene transition. A winter rainfall drying between 4.26 and 3.97 kyr BP was caused by a reduction precipitation from Westerly

Disturbance, and therefore may be linked to the 4.2 ka event. A summer rainfall drying started at 3.97 kyr BP, had a more gradual onset, but lasted for several centuries, if not permanently. This second drying was caused by a reduction in summer monsoon rainfall due to a global shift in the mean state of the tropics, possibly via an increase in El Niño event frequency. The Double Drying hypothesis has two important consequences for the climatic context of the Harappan civilization. First, it may solve the cropping paradox, where the Harappan shifted from winter to summer crops during the Late Mature phase. Second, sequential winter and summer dryings fit the pattern of Harappan site abandonment.

The findings presented here have implications for the attribution of the 4.2 ka event as a global climatic event. While some individual records from the Indian Ocean basin show locally significant climate excursions contemporaneous with the 4.2 ka event, when viewed basin wide the event has little regional coherence nor is it of unusual severity at most sites. The 4.2 ka event therefore had limited impact on tropical monsoonal rainfall around the Indian Ocean basin. Previous studies may have falsely attributed low latitude, low frequency climate variability to the 4.2 ka event when there are other significant changes in the tropical climate system at similar times. We propose that the 4.2 ka event may have a more limited geographical impact than is commonly assumed.

Code availability

This study uses the MC-PCA code of (Deininger et al., 2017). The MATLAB code is available from the original authors, as per the acknowledgments statement of the original manuscript. The insolation curve was calculated using The Climate Data Toolbox for MATLAB (Greene et al., 2019) and the daily insolation function originally by Eisenman and Huybers (2006).

Author contributions

NS conceived the study, ran data analysis, and was primarily responsible for writing the manuscript. SJB, DM and LRG provided guidance on project direction, discussion of findings and helped write and edit the manuscript. LR, PF and BT contributed to the development and interpretation of the records from Madagascar, and contributed to manuscript editing.

Declaration of competing interest

The authors declare that they have no known competing financial interests or personal relationships that could have appeared to influence the work reported in this paper.

Data availability

Principal Component Analysis results are available at the NOAA Paleoclimatology Database: https://www.ncdc.noaa.gov/paleo/study/37021 and from the authors (nick.scroxton@mu.ie). Speleothem $\delta^{18}O$ records are available from the SISAL database with entity IDs: Oman Q5 (351), India SAH (478), Sumatra TA12-2 (436), Rodrigues LAVI4 (369), Borneo BA03 (238), Jeita-1 (58), Uluu2 (437), Mawmluh KM-A (61), Mawmluh ML.1 (476), Mawmluh ML.2 (477) and Buca della Renella RL4 (381). The Australian stalagmite data is a composite of individual records available in the SISAL database with site ID 155. The new Anjohikely AK1 data is available at https://www.ncdc.noaa.gov/paleo/study/37062, and has been submitted to the SISAL database for future release. Mg/Ca and $\delta^{18}O$ data from Gol-E-Zard GZ14-1 is available from https://doi.org/10.1073/pnas.1808103115. Data from sediment core 63KA is available from http://eprints.esc.cam.ac.uk/4371/. Data from sediment core SO130-289KL is available from the Pangaea database with ID: 815851. Data from Neor Lake is available from https://doi.org/10.1016/j.quascirev.2015.07.006. The Harappan site radiocarbon database is from Sengupta et al., 2020.

Acknowledgements

NS, SJB and DM acknowledge support from NSF award AGS-1702891/1702691, LRG and SJB from NSF award BCS-1750598 and DM from NSF award EAR-1439559 and the MIT Ferry Fund. Fieldwork in northwest Madagascar was conducted under a collaborative accord for paleobiological research between the University of Antananarivo (Département de Paléontologie et d'Anthropologie Biologique) and the University of Massachusetts Amherst (Department of Anthropology); collaborative work was further supported under a second accord for paleobiological and paleoclimatological research between the University of Antananarivo (Mention Bassins sédimentaires, Evolution, Conservation) and the University of Massachusetts Amherst (Departments of Anthropology and Geosciences). The research was sanctioned by the Madagascar Ministry of Mines, the Ministry of Education, and the Ministry of Arts and Culture. The authors would like to thank David Hodell, Stacy Carolin and Alena Giesche at the University of Cambridge for their feedback over four years of project development.

Appendix A. Supplementary data

Supplementary data to this article can be found online at https://doi.org/10.1016/j.quascirev.2022.107837.

References

Abram, N.J., Gagan, M.K., Liu, Z., Hantoro, W.S., McCulloch, M.T., Suwargadi, B.W., 2007. Seasonal characteristics of the Indian Ocean Dipole during the Holocene epoch. Nature 445 (7125), 299–302. https://doi.org/10.1038/nature05477.

Anchukaitis, K.J., Tierney, J.E., 2012. Identifying coherent spatiotemporal modes in time-uncertain proxy paleoclimate records. Clim. Dynam. 41 (5–6), 1291–1306. https://doi.org/10.1007/s00382-012-1483-0.

Berkelhammer, M., Sinha, A., Stott, L., Cheng, H., Pausata, F.S.R., Yoshimura, K., 2012. In: Giosan, L., Fuller, D.Q., Nicoll, K., Flad, R.K., Clift, P.D. (Eds.), An Abrupt Shift in the Indian Monsoon 4000 Years Ago. American Geophysical Union (AGU), Washington, D. C., pp. 75–88

Bini, M., Zanchetta, G., Perşoiu, A., Cartier, R., Catala, A., Cacho, I., Dean, J.R., Di Rita, F., Drysdale, R.N., Finné, M., Isola, I., Jalali, B., Lirer, F., Magri, D., Masi, A., Marks, L., Mercuri, A.M., Peyron, O., Sadori, L., Sicre, M.-A., Welc, F., Zielhofer, C., Brisset, E., 2019. The 4.2 ka BP Event in the Mediterranean region: an overview. Clim. Past 15 (2), 555–577. https://doi.org/10.5194/cp-15-555-2019.

Booth, R.K., Jackson, S.T., Forman, S.L., Kutzbach, J.E., Bettis Iii, E.A., Kreigs, J., Wright, D.K., 2005. A severe centennial-scale drought in midcontinental North America 4200 years ago and apparent global linkages. Holocene 15 (3), 321–328. https://doi.org/10.1191/0959683605hl825ft.

Burstyn, Y., Martrat, B., Lopez, J.F., Iriarte, E., Jacobson, M.J., Lone, M.A., Deininger, M., 2019. Speleothems from the Middle East: an example of water limited environments in the SISAL database. Quaternary 216. https://doi.org/10.3390/quat2020016.

Butzer, K.W., Endfield, G.H., 2012. Critical perspectives on historical collapse. Proc. Natl. Acad. Sci. U.S.A. 109 (10), 3628–3631. https://doi.org/10.1073/pnas.1114772109.

Cai, Y., Zhang, H., Cheng, H., An, Z., Edwards, R.L., Wang, X., Tan, L., Liang, F., Wang, J., Kelly, M., 2012. The Holocene Indian monsoon variability over the southern Tibetan Plateau and its teleconnections. Earth Planet Sci. Lett. 335, 135–144.

Cannon, F., Carvalho, L.M.V., Jones, C., Bookhagen, B., 2015. Multi-annual variations in winter westerly disturbance activity affecting the Himalaya. Clim. Dynam. 44 (1–2), 441–455. https://doi.org/10.1007/s00382-014-2248-8.

Carolin, S.A., Walker, R.T., Day, C.C., Ersek, V., Sloan, R.A., Dee, M.W., Talebian, M., Henderson, G.M., 2019. Precise timing of abrupt increase in dust activity in the Middle East coincident with 4.2 ka social change. Proc. Natl. Acad. Sci. U.S.A. 116 (1), 67–72. https://doi.org/10.1073/pnas.1808103115.

Chen, S., Hoffmann, S.S., Lund, D.C., Cobb, K.M., Emile-Geay, J., Adkins, J.F., 2016. A high-resolution speleothem record of western equatorial Pacific rainfall: implications for Holocene ENSO evolution. Earth Planet Sci. Lett. 442, 61–71. https://doi.org/10.1016/j.epsl.2016.02.050.

Cookson, E., Hill, D.J., Lawrence, D., 2019. Impacts of long term climate change during the collapse of the Akkadian Empire. J. Archaeol. Sci. 1061–1069. https://

doi.org/10.1016/j.jas.2019.03.009.
de Boer, E.J., Tjallingii, R., Vélez, M.I., Rijsdijk, K.F., Vlug, A., Reichart, G.-J., Prendergast, A.L., de Louw, P.G.B., Florens, F.B.V., Baider, C., Hooghiemstra, H., 2014. Climate variability in the SW Indian Ocean from an 8000-yr long multi-proxy record in the Mauritian lowlands shows a middle to late Holocene shift from negative IOD-state to ENSO-state. Quat. Sci. Rev. 86, 175–189. https://doi.org/10.1016/j.quascirev.2013.12.026.
Deininger, M., McDermott, F., Mudelsee, M., Werner, M., Frank, N., Mangini, A., 2017. Coherency of late Holocene European speleothem δ18O records linked to North Atlantic Ocean circulation. Clim. Dynam. 49 (1), 595–618. https://doi.org/10.1007/s00382-016-3360-8.
deMenocal, P.B., 2001. Cultural responses to climate change during the late Holocene. Science 292 (5517), 667–673. https://doi.org/10.1126/science.1059287.
Denniston, R.F., Wyrwoll, K.-H., Polyak, V.J., Brown, J.R., Asmerom, Y., Wanamaker Jr., A.D., LaPointe, Z., Ellerbroek, R., Barthelmes, M., Cleary, D., Cugley, J., Woods, D., Humphreys, W.F., 2013. A Stalagmite record of Holocene Indonesian–Australian summer monsoon variability from the Australian tropics. Quat. Sci. Rev. 78, 155–168. https://doi.org/10.1016/j.quascirev.2013.08.004.
Deplazes, G., Lückge, A., Peterson, L.C., Timmermann, A., Hamann, Y., Hughen, K.A., Röhl, U., Laj, C., Cane, M.A., Sigman, D.M., Haug, G.H., 2013. Links between tropical rainfall and North Atlantic climate during the last glacial period. Nat. Geosci. 6 (3), 213–217. https://doi.org/10.1038/ngeo1712.
Dimri, A.P., Niyogi, D., Barros, A.P., Ridley, J., Mohanty, U.C., Yasunari, T., Sikka, D.R., 2015. Western disturbances: a review. Rev. Geophys. 53 (2), 225–246. https://doi.org/10.1002/2014RG000460.
Dixit, Y., Hodell, D.A., Petrie, C.A., 2014. Abrupt weakening of the summer monsoon in northwest India 4100 yr ago. Geology 42 (4), 339–342. https://doi.org/10.1130/G35236.1.
Dixit, Y., Hodell, D.A., Giesche, A., Tandon, S.K., Gázquez, F., Saini, H.S., Skinner, L.C., Mujtaba, S.A.I., Pawar, V., Singh, R.N., Petrie, C.A., 2018. Intensified summer monsoon and the urbanization of Indus Civilization in northwest India. Sci. Rep. 8 (1), 4225. https://doi.org/10.1038/s41598-018-22504-5.
Djamali, M., De Beaulieu, J.-L., Miller, N.F., Andrieu-Ponel, V., Ponel, P., Lak, R., Sadeddin, N., Akhani, H., Fazeli, H., 2009. Vegetation history of the SE section of the Zagros Mountains during the last five millennia; a pollen record from the Maharlou Lake, Fars Province, Iran. Veg. Hist. Archaeobotany 18 (2), 123–136. https://doi.org/10.1007/s00334-008-0178-2.
Dutt, S., Gupta, A.K., Wünnemann, B., Yan, D., 2018. A long arid interlude in the Indian summer monsoon during ~4,350 to 3,450 cal. yr BP contemporaneous to displacement of the Indus valley civilization. Quat. Int. 482, 83–92. https://doi.org/10.1016/j.quaint.2018.04.005.
Enzel, Y., Bookman, R., Sharon, D., Gvirtzman, H., Dayan, U., Ziv, B., Stein, M., 2003. Late Holocene climates of the Near East deduced from Dead Sea level variations and modern regional winter rainfall. Quat. Res. 60, 263–273. https://doi.org/10.1016/j.yqres.2003.07.011.
Fleitmann, D., Burns, S.J., Mudelsee, M., Neff, U., Kramers, J., Mangini, A., Matter, A., 2003. Holocene forcing of the Indian monsoon recorded in a stalagmite from southern Oman. Science 300 (5626), 1737–1739. https://doi.org/10.1126/science.1083130.
Fleitmann, D., Burns, S.J., Mangini, A., Mudelsee, M., Kramers, J., Villa, I., Neff, U., Al-Subbary, A.A., Buettner, A., Hippler, D., Matter, A., 2007. Holocene ITCZ and Indian monsoon dynamics recorded in stalagmites from Oman and Yemen (Socotra). Quat. Sci. Rev. 26 (1), 170–188. https://doi.org/10.1016/j.quascirev.2006.04.012.
Gagan, M.K., Hendy, E.J., Haberle, S.G., Hantoro, W.S., 2004. Post-glacial evolution of the indo-pacific warm pool and El nino-southern oscillation. Quat. Int. 118, 127–143. https://doi.org/10.1016/S1040-6182(03)00134-4.
Gangal, K., Vahia, M.N., Adhikari, R., 2010. Spatio-temporal analysis of the Indus urbanization. Curr. Sci. 98 (6), 846–852. https://doi.org/10.2307/24109857.
Giesche, A., Staubwasser, M., Petrie, C., Hodell, D., 2019. Indian winter and summer monsoon strength over the 4.2 ka BP event in foraminifer isotope records from the Indus River delta in the Arabian Sea. Clim. Past 15 (1), 73–90. https://doi.org/10.5194/cp-15-73-2019.
Giosan, L., Clift, P.D., Macklin, M.G., Fuller, D.Q., Constantinescu, S., Durcan, J.A., Stevens, T., Duller, G.A.T., Tabrez, A.R., Gangal, K., Adhikari, R., Alizai, A., Filip, F., VanLaningham, S., Syvitski, J.P.M., 2012. Fluvial landscapes of the Harappan civilization. Proc. Natl. Acad. Sci. U.S.A. 109 (26), E1688–E1694. https://doi.org/10.1073/pnas.1112743109.
Giosan, L., Orsi, W.D., Coolen, M., Wuchter, C., Dunlea, A.G., Thirumalai, K., Munoz, S.E., Clift, P.D., Donnelly, J.P., Galy, V., Fuller, D.Q., 2018. Neoglacial climate anomalies and the Harappan metamorphosis. Clim. Past 14 (11), 1669–1686. https://doi.org/10.5194/cp-14-1669-2018.
Greene, C.A., Thirumalai, K., Kearney, K.A., Delgado, J.M., Schwanghart, W., Wolfenbarger, N.S., Thyng, K.M., Gwyther, D.E., Gardner, A.S., Blankenship, D.D., 2019. The climate data toolbox for MATLAB. G-cubed 20 (7), 3774–3781. https://doi.org/10.1029/2019GC008392.
Gupta, A.K., Anderson, D.M., Overpeck, J.T., 2003. Abrupt changes in the asian southwest monsoon during the Holocene and their links to the north atlantic ocean. Nature 421 (6921), 354–357. https://doi.org/10.1038/nature01340.
Gupta, A.K., Anderson, D.M., Pandey, D.N., Singhvi, A.K., 2006. Adaptation and human migration, and evidence of agriculture coincident with changes in the Indian summer monsoon during the Holocene. Curr. Sci. 1082–1090.
Gupta, A.K., Dutt, S., Das, M., Singh, R.K., 2021. Teleconnection between Arctic climate and tropical Indian monsoon during the Holocene. In: Understanding Present and Past Arctic Environments. Elsevier, pp. 117–136.
Hamzeh, M.A., Gharaie, M.H.M., Lahijani, H.A.K., Djamali, M., Harami, R.M., Beni, A.N., 2016. Holocene hydrological changes in SE Iran, a key region between Indian Summer Monsoon and Mediterranean winter precipitation zones, as revealed from a lacustrine sequence from Lake Hamoun. Quat. Int. 408, 25–39. https://doi.org/10.1016/j.quaint.2015.11.011.
Haug, G.H., Hughen, K.A., Sigman, D.M., Peterson, L.C., Röhl, U., 2001. Southward migration of the intertropical convergence zone through the Holocene. Science 293 (5533), 1304–1308. https://doi.org/10.1126/science.1059725.
Helama, S., Oinonen, M., 2019. Exact dating of the Meghalayan lower boundary based on high-latitude tree-ring isotope chronology. Quat. Sci. Rev. 214, 178–184. https://doi.org/10.1016/j.quascirev.2019.04.013.
Höflmayer, F., 2017. In: Höflmayer, F. (Ed.), The Late Third Millennium B.C. In the Ancient Near East and Eastern Mediterranean: A Time of Collapse and Transformation. Oriental Institute Seminars, pp. 1–30.
Huang, Y., Wu, B., Li, T., Zhou, T., Liu, B., 2019. Interdecadal Indian Ocean basin mode driven by interdecadal Pacific oscillation: a season-dependent growth mechanism. J. Clim. 32 (7), 2057–2073.
Huybers, P., 2006. Early Pleistocene glacial cycles and the integrated summer insolation forcing. Science 313 (5786), 508–511. https://doi.org/10.1126/science.1125249.
Kaniewski, D., Paulissen, E., Van Campo, E., Al-Maqdissi, M., Bretschneider, J., Van Lerberghe, K., 2008. Middle East coastal ecosystem response to middle-to-late Holocene abrupt climate changes. Proc. Natl. Acad. Sci. U.S.A. 105 (37), 13941–13946. https://doi.org/10.1073/pnas.0803533105.
Kaniewski, D., Marriner, N., Cheddadi, R., Guiot, J., Campo, E.V., 2018. The 4.2 ka BP event in the Levant. Clim. Past 14 (10), 1529–1542. https://doi.org/10.5194/cp-14-1529-2018.
Kathayat, G., Cheng, H., Sinha, A., Yi, L., Li, X., Zhang, H., Li, H., Ning, Y., Edwards, R.L., 2017. The Indian monsoon variability and civilization changes in the Indian subcontinent. Sci. Adv. 3 (12), e1701296. https://doi.org/10.1126/sciadv.1701296.
Kathayat, G., Cheng, H., Sinha, A., Berkelhammer, M., Zhang, H., Duan, P., Li, H., Li, X., Ning, Y., Edwards, R.L., 2018. Evaluating the timing and structure of the 4.2 ka event in the Indian summer monsoon domain from an annually resolved speleothem record from Northeast India. Clim. Past 14 (12), 1869–1879. https://doi.org/10.5194/cp-14-1869-2018.
Kaushal, R., Ghosh, P., Pokharia, A.K., 2019. Stable isotopic composition of rice grain organic matter marking an abrupt shift of hydroclimatic condition during the cultural transformation of Harappan civilization. Quat. Int. 512, 144–154. https://doi.org/10.1016/j.quaint.2019.04.017.
Kotlia, B.S., Singh, A.K., Joshi, L.M., Dhaila, B.S., 2015. Precipitation variability in the Indian central Himalaya during last ca. 4,000 years inferred from a speleothem record: impact of Indian summer monsoon (ISM) and westerlies. Quat. Int. 371, 244–253. https://doi.org/10.1016/j.quaint.2014.10.066.
Kotlia, B.S., Singh, A.K., Joshi, L.M., Bisht, K., 2018. Precipitation variability over Northwest Himalaya from ~4.0 to 1.9 ka BP with likely impact on civilization in the foreland areas. J. Asian Earth Sci. 162, 148–159. https://doi.org/10.1016/j.jseaes.2017.11.025.
Lang, T.J., Barros, A.P., 2004. Winter storms in the central Himalayas. J. Meteorol. Soc. Japan 82 (3), 829–844, 1.
Li, H., Cheng, H., Sinha, A., Kathayat, G., Spötl, C., André, A.A., Meunier, A., Biswas, J., Duan, P., Ning, Y., Edwards, R.L., 2018. Hydro-climatic variability in the southwestern Indian Ocean between 6000 and 3000 years ago. Clim. Past 14 (12), 1881–1891. https://doi.org/10.5194/cp-14-1881-2018.
MacDonald, G., 2011. Potential influence of the Pacific Ocean on the Indian summer monsoon and Harappan decline. Quat. Int. 229 (1–2), 140–148. https://doi.org/10.1016/j.quaint.2009.11.012&hl=en&num=1&as_sdt=0,5.
Madella, M., Fuller, D.Q., 2006. Palaeoecology and the harappan civilisation of south asia: a reconsideration. Quat. Sci. Rev. 25 (11–12), 1283–1301. https://doi.org/10.1016/j.quascirev.2005.10.012.
Marchant, R., Hooghiemstra, H., 2004. Rapid environmental change in African and South American tropics around 4000 years before present: a review. Earth Sci. Rev. 66 (3–4), 217–260. https://doi.org/10.1016/j.earscirev.2004.01.003.
Mayewski, P.A., Rohling, E.E., Stager, J.C., Karlén, W., Maasch, K.A., Meeker, L.D., Meyerson, E.A., Gasse, F., van Kreveld, S., Holmgren, K., Lee-Thorp, J., Rosqvist, G., Rack, F., Staubwasser, M., Schneider, R.R., Steig, E.J., 2004. Holocene climate variability. Quat. Res. 62 (3), 243–255. https://doi.org/10.1016/j.yqres.2004.07.001.
Mehrotra, N., Shah, S.K., Basavaiah, N., Laskar, A.H., Yadava, M.G., 2018. Resonance of the '4.2ka event' and terminations of global civilizations during the Holocene, in the palaeoclimate records around PT Tso Lake, Eastern Himalaya. Quat. Int. 507, 206–216. https://doi.org/10.1016/j.quaint.2018.09.027.
Mehterian, S., Pourmand, A., Sharifi, A., Lahijani, H.A.K., Naderi, M., Swart, P.K., 2017. Speleothem records of glacial/interglacial climate from Iran forewarn of future Water Availability in the interior of the Middle East. Quat. Sci. Rev. 164, 187–198. https://doi.org/10.1016/j.quascirev.2017.03.028.
Midhuna, T.M., Kumar, P., Dimri, A.P., 2020. A new Western Disturbance Index for the Indian winter monsoon. J. Earth Syst. Sci. 129 (1), 59. https://doi.org/10.1007/s12040-019-1324-1.
Mooley, D.A., Parthasarathy, B., 1983. Indian summer monsoon and El Nino. Pure Appl. Geophys. 121 (2), 339–352. https://doi.org/10.1007/BF02590143.
Morrill, C., Overpeck, J.T., Cole, J.E., Liu, K.-b., Shen, C., Tang, L., 2006. Holocene variations in the Asian monsoon inferred from the geochemistry of lake sediments in central Tibet. Quat. Res. 65 (2), 232–243. https://doi.org/10.1016/j.yqres.2005.02.014.

Mudelsee, M., 2000. Ramp function regression: a tool for quantifying climate transitions. Comput. Geosci. 26 (3), 293–307. https://doi.org/10.1016/s0098-3004(99)00141-7.
Mudelsee, M., 2013. Climate Time Series Analysis. Springer, Heidelberg.
Nakamura, A., Yokoyama, Y., Maemoku, H., 2016. Weak monsoon event at 4.2 ka recorded in sediment from Lake Rara, Himalayas. Quat. Int. 397, 349–359. https://doi.org/10.1016/j.quaint.2015.05.053.
Olsen, J., Anderson, N.J., Knudsen, M.F., 2012. Variability of the north atlantic oscillation over the past 5,200 years. Nat. Geosci. 5 (11), 808–812. https://doi.org/10.1038/ngeo1589.
Petrie, C.A., Bates, J., Higham, T., Singh, R.N., 2016. Feeding ancient cities in South Asia: dating the adoption of rice, millet and tropical pulses in the Indus civilisation. Antiquity 90 (354), 1489–1504. https://doi.org/10.15184/aqy.2016.210.
Petrie, C.A., Bates, J., 2017. 'Multi-cropping', intercropping and adaptation to variable environments in Indus South Asia. J. World Prehist. 30 (2), 81–130. https://doi.org/10.1007/s10963-017-9101-z.
Petrie, C.A., Singh, R.N., Bates, J., Dixit, Y., French, C.A.I., Hodell, D.A., Jones, P.J., Lancelotti, C., Lynam, F., Neogi, S., Pandey, A.K., Parikh, D., Pawar, V., Redhouse, D.I., Singh, D.P., 2017. Adaptation to variable environments, resilience to climate change: investigating land, water and settlement in Indus northwest India. Curr. Anthropol. 58 (1), 1–30. https://doi.org/10.1086/690112.
Phadtare, N.R., 2000. Sharp decrease in summer monsoon strength 4000–3500 cal yr B.P. In the central higher Himalaya of India based on pollen evidence from alpine peat. Quat. Res. 53 (1), 122–129. https://doi.org/10.1006/qres.1999.2108.
Pokharia, A.K., Kharakwal, J.S., Srivastava, A., 2014. Archaeobotanical evidence of millets in the Indian subcontinent with some observations on their role in the Indus civilization. J. Archaeol. Sci. 42, 442–455.
Pokharia, A.K., Agnihotri, R., Sharma, S., Bajpai, S., Nath, J., Kumaran, R.N., Negi, B.C., 2017. Altered cropping pattern and cultural continuation with declined prosperity following abrupt and extreme arid event at~ 4,200 yrs BP: evidence from an Indus archaeological site Khirsara, Gujarat, western India. PLoS One 12 (10). https://doi.org/10.1371/journal.pone.0185684.
Possehl, G.L., 1993. The date of Indus urbanization: a proposed chronology for the pre-urban and urban harappan phases. South Asian Archaeology 231–249, 1991.
Possehl, G.L., 1997. Climate and the eclipse of the ancient cities of the Indus. In: Third Millennium BC Climate Change and Old World Collapse, vol. 193. Springer, Berlin, Heidelberg.
Possehl, G.L., 2002. The Indus Civilization: A Contemporary Perspective. Rowman Altamira.
Prasad, S., Anoop, A., Riedel, N., Sarkar, S., Menzel, P., Basavaiah, N., Krishnan, R., Fuller, D., Plessen, B., Gaye, B., Röhl, U., Wilkes, H., Sachse, D., Sawant, R., Wiesner, M.G., Stebich, M., 2014. Prolonged monsoon droughts and links to Indo-Pacific warm pool: a Holocene record from Lonar Lake, central India. Earth Planet Sci. Lett. 391, 171–182. https://doi.org/10.1016/j.epsl.2014.01.043.
Ronay, E.R., Breitenbach, S.F.M., Oster, J.L., 2019. Sensitivity of speleothem records in the Indian Summer Monsoon region to dry season infiltration. Sci. Rep. 9 (1), 1–10. https://doi.org/10.1038/s41598-019-41630-2.
Sandeep, K., Shankar, R., Warrier, A.K., Yadava, M.G., Ramesh, R., Jani, R.A., Weijian, Z., Xuefeng, L., 2017. A multi-proxy lake sediment record of Indian summer monsoon variability during the Holocene in southern India. Palaeogeogr. Palaeoclimatol. Palaeoecol. 476, 1–14. https://doi.org/10.1016/j.palaeo.2017.03.021.
Schneider, T., Bischoff, T., Haug, G.H., 2014. Migrations and dynamics of the intertropical convergence zone. Nature 513 (7516), 45–53. https://doi.org/10.1038/nature13636.
Schug, G.R., Blevins, K.E., Cox, B., Gray, K., Mushrif-Tripathy, V., 2013. Infection, disease, and biosocial processes at the end of the Indus Civilization. PLoS One 8 (12), e84814.
Scroxton, N., Burns, S.J., McGee, D., Godfrey, L.R., Ranivoharimanana, L., Faina, P., Tiger, B.H., 2023. Hydroclimate variability in the Madagascar and Southeast African summer monsoons at the Mid- to Late-Holocene transition. Quat. Sci. Rev. 107874. https://doi.org/10.1016/j.quascirev.2022.107874.
Sengupta, T., Deshpande Mukherjee, A., Bhushan, R., Ram, F., Bera, M.K., Raj, H., Dabhi, A.J., Bisht, R.S., Rawat, Y.S., Bhattacharya, S.K., Juyal, N., Sarkar, A., 2020. Did the Harappan settlement of Dholavira (India) collapse during the onset of Meghalayan stage drought. J. Quat. Sci. 35 (3), 382–395. https://doi.org/10.1002/jqs.3178.
Sharifi, A., Pourmand, A., Canuel, E.A., Ferer-Tyler, E., Peterson, L.C., Aichner, B., Feakins, S.J., Daryaee, T., Djamali, M., Beni, A.N., 2015. Abrupt climate variability since the last deglaciation based on a high-resolution, multi-proxy peat record from NW Iran: the hand that rocked the Cradle of Civilization. Quat. Sci. Rev. 123, 215–230. https://doi.org/10.1016/j.quascirev.2015.07.006.
Singh, G., 1971. The Indus Valley culture: seen in the context of post-glacial climatic and ecological studies in north-west India. Archaeol. Phys. Anthropol. Ocean. 6 (2), 177–189.
Singh, G., Wasson, R.J., Agrawal, D.P., 1990. Vegetational and seasonal climatic changes since the last full glacial in the Thar Desert, northwestern India. Rev. Palaeobot. Palynol. 64 (1), 351–358. https://doi.org/10.1016/0034-6667(90)90151-8.
Staubwasser, M., Sirocko, F., Grootes, P.M., Segl, M., 2003. Climate change at the 4.2 ka BP termination of the Indus valley civilization and Holocene south Asian monsoon variability. Geophys. Res. Lett. 30 (8), 155. https://doi.org/10.1029/2002GL016822.
Staubwasser, M., Weiss, H., 2006. Holocene climate and cultural evolution in late prehistoric–early historic west asia. Quat. Res. 66 (3), 372–387. https://doi.org/10.1016/j.yqres.2006.09.001.
Stevens, L.R., Ito, E., Schwalb, A., Jr, H.E.W., 2006. Timing of atmospheric precipitation in the Zagros Mountains inferred from a multi-proxy record from Lake Mirabad, Iran. Quat. Res. 66, 494–500. https://doi.org/10.1016/j.yqres.2006.06.008.
Syed, F.S., Giorgi, F., Pal, J.S., King, M.P., 2006. Effect of remote forcings on the winter precipitation of central southwest Asia part 1: observations. Theor. Appl. Climatol. 86 (1–4), 147–160. https://doi.org/10.1007/s00704-005-0217-1.
Thompson, L.G., Tandong, Y., Davis, M.E., Mosley-Thompson, E., Mashiotta, T.A., Lin, P.-N., Mikhalenko, V.N., Zagorodnov, V.S., 2006. Holocene climate variability archived in the Puruogangri ice cap on the central Tibetan Plateau. Ann. Glaciol. 43, 61–69. https://doi.org/10.3189/172756406781812357.
Tierney, J.E., deMenocal, P.B., 2013. Abrupt shifts in horn of Africa hydroclimate since the last glacial maximum. Science 342 (6160), 843–846. https://doi.org/10.1126/science.1240411.
Toth, L.T., Aronson, R.B., Vollmer, S.V., Hobbs, J.W., Urrego, D.H., Cheng, H., Enochs, I.C., Combosch, D.J., Van Woesik, R., Macintyre, I.G., 2012. ENSO drove 2500-year collapse of eastern Pacific coral reefs. Science 337 (6090), 81–84. https://doi.org/10.1126/science.1221168.
Toth, L.T., Aronson, R.B., 2019. The 4.2 ka event, ENSO, and coral reef development. Clim. Past 15 (1), 105–119. https://doi.org/10.5194/cp-15-105-2019.
Trivedi, A., Chauhan, M.S., 2009. Holocene vegetation and climate fluctuations in northwest Himalaya, based on pollen evidence from Surinsar Lake, Jammu region, India. J. Geol. Soc. India 74 (3), 402–412. https://doi.org/10.1007/s12594-009-0142-5.
Vahia, M.N., Yadav, N., 2011. Reconstructing the history of harappan civilization. Soc. Evol. Hist 10 (2), e9506. https://doi.org/10.1371/journal.pone.0009506.
Walker, M., Head, M.H., Berklehammer, M., Bjorck, S., Cheng, H., Cwynar, L., Fisher, D., Gkinis, V., Long, A., Lowe, J., Newnham, R., Rasmussen, S.O., Weiss, H., 2018. Formal ratification of the subdivision of the Holocene series/epoch (quaternary system/period): two new global boundary Stratotype sections and points (GSSPs) and three new stages/subseries. Episodes 41 (4), 213–223. https://doi.org/10.18814/epiiugs/2018/018016.
Wang, J., Sun, L., Chen, L., Xu, L., Wang, Y., Wang, X., 2016. The abrupt climate change near 4,400 yr BP on the cultural transition in Yuchisi, China and its global linkage. Sci. Rep., 627723
Wang, L., Brook, G.A., Burney, D.A., Voarintsoa, N.R.G., Liang, F., Cheng, H., Edwards, R.L., 2019. The African Humid Period, rapid climate change events, the timing of human colonization, and megafaunal extinctions in Madagascar during the Holocene: evidence from a 2m Anjohibe Cave stalagmite. Quat. Sci. Rev. 210, 136–153. https://doi.org/10.1016/j.quascirev.2019.02.004.
Wang, S., Ge, Q., Wang, F., Wen, X., Huang, J., 2013. Abrupt climate changes of Holocene. Chin. Times 23 (1), 1–12. https://doi.org/10.1007/s11769-013-0591-z.
Wanner, H., Solomina, O., Grosjean, M., Ritz, S.P., Jetel, M., 2011. Structure and origin of Holocene cold events. Quat. Sci. Rev. 30 (21–22), 3109–3123. https://doi.org/10.1016/j.quascirev.2011.07.010.
Watanabe, T.K., Watanabe, T., Yamazaki, A., Pfeiffer, M., 2019. Oman corals suggest that a stronger winter shamal season caused the Akkadian Empire (Mesopotamia) collapse. Geology 47 (12), 1141–1145. https://doi.org/10.1130/G46604.1.
Weiss, H., Bradley, R.S., 2001. What drives societal collapse? Science 291 (5504), 609–610. https://doi.org/10.1126/science.1058775.
Wright, R., Bryson, R., Schuldenrein, J., 2008. Water supply and history: harappa and the Beas regional survey. Antiquity 82 (315), 37–48. https://doi.org/10.1017/s0003598x00096423.
Wünnemann, B., Demske, D., Tarasov, P., Kotlia, B.S., Reinhardt, C., Bloemendal, J., Diekmann, B., Hartmann, K., Krois, J., Riedel, F., 2010. Hydrological evolution during the last 15 kyr in the Tso Kar lake basin (Ladakh, India), derived from geomorphological, sedimentological and palynological records. Quat. Sci. Rev. 29 (9–10), 1138–1155. https://doi.org/10.1016/j.quascirev.2010.02.017.
Wurtzel, J.B., Abram, N.J., Lewis, S.C., Bajo, P., Hellstrom, J.C., Troitzsch, U., Heslop, D., 2018. Tropical Indo-Pacific hydroclimate response to North Atlantic forcing during the last deglaciation as recorded by a speleothem from Sumatra, Indonesia. Earth Planet Sci. Lett. 492, 264–278. https://doi.org/10.1016/j.epsl.2018.04.001.
Yadav, R.K., Kumar, K.R., Rajeevan, M., 2012. Characteristic features of winter precipitation and its variability over northwest India. J. Earth Syst. Sci. 121 (3), 611–623. https://doi.org/10.1007/s12040-012-0184-8.
Yan, M., Liu, J., 2019. Physical processes of cooling and mega-drought during the 4.2 ka BP event: results from TraCE-21ka simulations. Clim. Past 15 (1), 265–277. https://doi.org/10.5194/cp-15-265-2019.